UNIVERSITY OF MANITOBA

SIMPLIFIED TECHNIQUES TO DETERMINE THE RESPONSE OF STRUCTURES TO TRANSIENT LOADS

by

BALRAM ARYA

SUBMITTED TO THE FACULTY OF GRADUATE STUDIES
IN PARTIAL FULFILMENT OF THE REQUIREMENTS FOR THE DEGREE
OF MASTER OF SCIENCE

DEPARTMENT OF MECHANICAL ENGINEERING

WINNIPEG, MANITOBA

February, 1972

ABSTRACT

This thesis is divided into two parts. In the first part, simple design curves are developed to determine the possibility of instantaneous damage to wall-like structural components and of people's annoyance due to structural vibrations created by sonic booms. A design curve for possible damage is obtained using a damage threshold criterion involving a peak velocity of 4.5 in/sec. This criterion has been established experimentally from blasting operations. Then the design curve is used to determine the magnitude of those sonic booms which are likely to cause damage to single-thickness brick walls. The validity of the damage curve is checked by comparing the theoretical values with actual damage data observed in the field. A tentative criterion is employed for people's annoyance to vibrations caused by booms. It is given in terms of peak displacement versus frequency. Verification of the annoyance curves cannot be made at this time as relevant information is unavailable at present.

The accuracy of a method which reduces the number of unknown variables in structural dynamics is investigated in the second part. The aim of this technique is to preserve information relating to the lowest frequency modes. It is used here in determining approximate free and transient responses of a rectangular plate in bending. All edges of the plate are simply-supported as exact solutions exist for these edge conditions. The effect of eliminating different variables is assessed by comparing

the resulting lowest natural frequencies with exact values. Similarly, corresponding effects on the plate's transient response are estimated by comparison with exact results evaluated using the normal mode technique. Results indicate that acceptable displacements and velocities can be obtained when only a few of the original variables are retained. However, corresponding accelerations - being most sensitive to higher frequencies - may be unreliable.

ACKNOWLEDGEMENT

The author would like to express his appreciation to Dr. N. Popplewell for his helpful and inspiring supervision.

Further, the author is indebted to National Research Council of Canada for its financial support.

CONTENTS

NOTATION

Part I

ω	fundamental circular frequency, rad/sec.
s	ratio of total to positive pressure duration of sonic boom
τ	positive duration of sonic boom
r_1, r_2	rise time ratios of sonic booms (in Figure 1b, $r_1=t_R/\tau$, $r_2=t_1/\tau$)
$\alpha,\beta,\gamma,\lambda$	sonic boom parameters
p^+, p^-	positive and negative peak pressures respectively
t,σ	time
$x(t), \dot{x}(t)$	displacement and velocity respectively
$x_s, \dot{x}_s$	non-dimensionalizing displacement and velocity parameters respectively.
$x_n(t)$, $\dot{x}_n(t)$	non-dimensionalized displacement and velocity respectively.
$x_{max}, \dot{x}_{max}$	maximum displacement and velocity, respectively
daf	maximum non-dimensionalized response (called dynamic amplification factor)
$x_o, \dot{x}_o$	initial conditions of displacement and velocity respectively
$p(\sigma)$	arbitrary excitation
$p(\omega)$	fourier transform or frequency spectrum of $p(\sigma)$
$w(s\tau)$	displacement amplitude of free vibration

Part II

w	transverse displacement
$\underline{M}$	overall mass matrix
$\underline{M}_c$	constrained overall mass matrix
$\underline{M}_e$	element mass matrix
$\underline{M}^*$	reduced overall mass matrix
$\underline{K}$	overall stiffness matrix

$\underline{K}_c$	constrained overall stiffness matrix
$\underline{K}_e$	element stiffness matrix
$\underline{K}^*$	reduced overall stiffness matrix
$\{F\}$	overall forcing vector
$\{F\}_e$	element forcing vector
$\{F\}_c$	constrained overall forcing vector
$\{F\}^*$	reduced overall forcing vector
$\{w\}$	overall deflection vector
$\{w\}_e$	element deflection vector
$\{w\}_c$	constrained overall deflection vector
$\{w\}^*$	reduced overall deflection vector

General

a,b	dimensions of a rectangular wall or a plate
f	fundamental frequency, Hz
E	Young's modulus
k	stiffness
h	thickness
l	some standard length
g	acceleration due to gravity
ν	Poisson's ratio
I	cross sectional moment of inertia
$D=\frac{Eh^3}{12(1-\nu^2)}$	flexural rigidity
ρ_{ST}	surface density

Subscripts

x,y	partial derivatives with respect to x and y respectively
c	constrained
e	element
max	maximum

Symbols

{ }	vector matrix
—	square matrix
.	a dot denotes differentiation with respect to time

PART I

1.0 Introduction

The prospect of regular supersonic passenger-transport services has resulted in concern with the effects of sonic boom on people and buildings. A sonic boom is the pressure disturbance experienced on the ground when an aircraft flies overhead at a speed greater than that of sound. The form of the pressure-time history of the boom is described by a capital N for ideal atmospheric conditions (1). For actual conditions, however, deviations from this idealized form can occur due to atmospheric turbulence, ground absorption and reflections from buildings. Typical wave shapes which have been recorded in the field (2,3) are shown in Figure 1(a).

Information regarding the effects of sonic booms on structures is invaluable in preventing damage to buildings and reducing the annoyance of people within the buildings. The main purpose of this work is to construct simple design curves which can be used to assess the possibility of damage to wall-like components and of people's annoyance due to structural vibrations caused by sonic boom loading. Consequently, two types of information are required. Firstly, it is necessary to determine the damage and annoyance criteria in terms of a parameter like maximum stress or displacement. Then, secondly, the response of the structure which corresponds to the two criteria has to be evaluated. It has been established from blasting operations that a peak velocity of 4.5 in/sec often results in superficial damage to nearby structures (4). An

identical value of 4.5 in/sec is used to assess potential damage to structures from sonic booms,as the pressure wave produced by blasting operations is similar in nature to a sonic boom. There is no comparable criterion available at present, however, from which the annoyance of people when subjected to transient excitations can be determined. But Reiher and Meister (5) have established experimentally the levels of vibration at which people get irritated or annoyed for steady state conditions. These levels are given in terms of displacement amplitude, the amplitude varying with frequency (see Figure 7). This criterion is used to construct tentative curves for people's annoyance due to transient structural vibrations caused by sonic booms. When more information becomes available, the design curve can be modified, providing the new criterion is also given in terms of peak displacement.

To evaluate the peak displacement and velocity approximately, a wall-like component of a structure is idealized as an undamped linear oscillator. In this thesis only peak non-dimensionalized velocities of the idealized system are determined when the system is subjected to a sonic boom. Results for peak non-dimensionalized displacements of the same system and similar excitations have been obtained by Crocker and Hudson (6) and Cheng and Benveniste(7). These displacements are used directly to construct annoyance curves. Hereafter the non-dimensionalized peak displacement and velocity are known as the displacement and velocity daf, respectively. (Daf is the abbreviated form of dynamic amplification factor).

Results show that both the free motion displacement and velocity dafs are greater than corresponding dafs occurring during

forced motion for most values of τ/T (ratio of positive duration of sonic boom to fundamental period of the system). Hence, an alternative method which determines the free motion dafs in terms of the Fourier Transform of an arbitrary excitation is presented.

1.1 Idealization of the Structure

A typical three dimensional building is a flexible structure composed of many components. It can respond in many modes of vibration when subjected to an impact loading. Also, the dynamic characteristics of typical buildings can change with time due to cyclic changes in temperature, humidity and ageing of components (14). In this situation, it is clear that classical vibration theory must be based on severe assumptions and, thus, can only act as a guide to the likely trends of the structure's response. There are, however, a few specific elements such as walls which can be treated in a relatively simple fashion to produce useful results. A brief outline of previous work in this area is presented below. It forms the basis for the idealization of the structure.

Early and some later work (8,9) assumed that a structure was composed of a set of uncoupled components which vibrate in their own fundamental mode when excited by the boom. Thus, each component can be represented by the simplest model — an oscillator with discrete mass, stiffness and damping properties characteristic of that component - excited by a spatially concentrated transient force. Subsequently, components were considered to be independent beams or plates acted

upon by a distributed pressure wave. The wave's direction of propagation was assumed to be perpendicular to the span of the beam or plate (hereafter called normal incidence). Cheng and Benveniste (10) point out that the response of such idealizations is similar to that of a simple oscillator when the ratio of the boom's period, s_T, to the beam or plate's fundamental period, T, is in a range occurring for most practical situations (1/2 to 4). However, only displacements were taken into account and these, unlike accelerations, are not particularly sensitive to higher frequency modes.

The work was extended to the more generally representative situation of a sonic boom travelling over a plate (10, 11, 12, 13). Antisymmetric modes, which do not contribute to the plate's response when a wave is at normal incidence, are excited for this type of loading. It was shown that, as a result of the boom's convection, there is a critical velocity for every structural mode which causes resonance to occur in that particular mode. Although Cheng (12) developed an analytical solution, he simplified his final analysis considerably by using only the fundamental mode and a single speed of transverse corresponding to the resonant condition of this mode. Both Crocker (11) and Craggs (13) showed that the antisymmetric modes provide a significant contribution to the form of the overall response-time history although their effect is most marked on the plate's strains and accelerations.

Later, Popplewell (14,15) considered a structure as a box whose faces were not acting as independent plates. Thus, due to structural coupling, the effect of a force acting on one face could

be observed on other faces. Using three finite element models, a simple oscillator, a plate, and a box, Popplewell pointed out that reasonably accurate results could be obtained for displacements and velocities when a wall-like component of a structure is idealized as a simple linear oscillator with discretized mass and stiffness characteristic of the wall. Note that the assumption of linearity was considered acceptable for small sonic boom overpressures (1 to 2 lb/ft^2) which create small deformations in the structure. This analysis is simplified even further here by neglecting damping. The simplification will result in an overestimate of the peak displacements and velocities of the system and, hence, a conservative estimate of the sonic boom loads from the viewpoint of damage and annoyance of people within buildings.

1.2 Idealization of Sonic Booms

Figure 1(a) shows typical pressure-time histories of sonic booms which have been recorded in free field conditions (2,3). Reference (7) suggests that the most severe case of structural loading occurs when the direction of propagation of a sonic boom is normal to a face. Consequently, this is the case considered. Further simplications of the pressure-time histories are made so that the sonic boom can be described mathematically (see Figure 1(b)). These 'idealized' forms essentially reduce the low-amplitude, high frequency content of the boom which usually has negligible effect on the structure's response (14). To account for asymmetry in the pulse shape, a pulse length

parameter s (the ratio of the total to the positive duration of the boom) and a rise time parameter r_1 (the ratio of rise time, t_R, to the positive duration τ) are used to describe the sonic boom.

In reality, the form of the boom is modified when it travels over a structure. The significance of this modification is twofold. Firstly, waveforms observed experimentally over a full-scale structure indicate that the total duration of the sonic boom becomes less well-defined (17) due to ragging of the tail portion of the pressure signature. However, Warren (17) suggests that from the structural point of view this ragged tail portion does not contribute significantly to the response. Secondly, the form of the pressure-time history changes. These changes are caused by rarefaction, diffraction and reflection of the boom and formation of vortices at the edges of the structure. The exact features of these phenomena are unknown at present but are probably similar to those observed for a blast wave (18). Reference (19) points out that when the wave is at normal incidence, the front face of a structure would experience pressure "doubling" if the weak shock wave were reflected totally, its front remaining planar. However, due to the flexibility of the structure, energy is transmitted to the structure and the finite dimensions give rise to distortions of the wave front. Therefore the increase in pressure may not correspond exactly to pressure doubling. Reference (18) suggests that, in practice, an amplification of 1.4 to 1.5 occurs on the peak free field, positive pressure. Nevertheless, the effect of this increase is neglected in this thesis as reference (20) indicates that theoretical results for the response of a simple undamped oscillator

to an N type wave (Figure 1(b)) encompass all measured responses of large windows and vertical studs due to actual sonic boom loadings.

1.3 Method of Analysis

For an arbitrary excitation, $p(\sigma)$, the displacement $x(t)$, of an undamped linear oscillator is given by Duhamel's Integral (21) to be

$$x(t) = \frac{1}{m\omega} \int_0^t p(\sigma) \sin \omega(t-\sigma)\, d\sigma . \qquad 0 \leq \sigma \leq s\tau \qquad (1)$$

m and ω are the mass and natural circular frequency of the system, respectively and $s\tau$ is the total duration of the excitation.

The corresponding expression for the velocity, $\dot{x}(t)$, is

$$\dot{x}(t) = \frac{1}{m} \int_0^t p(\sigma) \cos \omega(t-\sigma)\, d\sigma . \qquad 0 \leq \sigma \leq s\tau \qquad (2)$$

The displacement and velocity during free motion (i.e. the motion after the termination of the excitation) are given as

$$\left.\begin{aligned} x(t) &= x_o \cos \omega t + \frac{\dot{x}_o}{\omega} \sin \omega t \qquad (3) \\ \text{and} \\ \dot{x}(t) &= -\omega x_o \sin \omega t + \dot{x}_o \cos \omega t \qquad (4) \end{aligned}\right\} \quad t \geq s\tau .$$

x_o and $\dot{x}_o$ are the displacement and velocity at time $t = s\tau$, respectively. They can be determined from equations (1) and (2).

Using the above equations, the velocity-time history of an undamped linear oscillator was derived for each of the idealized sonic booms shown in Figure 1(b). The resulting equations of motion

are given in Table 1.

Transient displacements are usually non-dimensionalized by dividing x(t) by the static deflection due to an identical peak load, $x_s = p^+/m\omega^2$ (7). To be consistent, the velocities are also given in non-dimensionalized form. In this case, however, the dividing factor is ωx_s, or $\dot{x}_s \equiv \omega x_s = p^+/m\omega$. For convenience, the non-dimensionalized forms of displacement and velocity are abbreviated as $x_n(t)$ and $\dot{x}_n(t)$, respectively. Their peaks are known as the dynamic amplification factor (daf).

1.4 Results and Discussion

This work deals with the instantaneous damage of a structure rather than cumulative damage over a period of time. Since the damage criterion is given in terms of the peak velocity of the structure, the peak velocity of the idealized system created by each sonic boom is of interest. This peak will occur during the time of application of the wave or in the first cycle of vibration after its termination. The analytical method of determining the absolute maximum velocity is to find the instants at which the maximum and minimum velocities occur by equating the acceleration to zero. Then the peak velocities can be obtained by evaluating the velocities at these instants. However, this can be a needlessly tedious task. An alternative but approximate method is employed whereby the velocity-time histories during forced motion and the first cycle of free vibration are computed using equations (2) and (4). Then the absolute maximum velocity during forced and

free motion are determined by comparing the velocities computed at different instants of time. A brief description and the FORTRAN listing of the computer program written to perform these operations are given in Appendix C. A time step equal to 1/100th of the sonic boom period is taken so that errors involved in computing the peak velocities will be sufficiently small for practical purposes.

The variations of the parameters considered in the computation are

τ/T	0 to 2.5
r_1	0 to 0.5
s	1.6 to 2.2.

These variations are considered representative of actual sonic booms (6). Furthermore the above range for τ/T is consistent with those values considered previously by Cheng and Benveniste (7).

The parameters are varied independently to determine their effect on the oscillator's peak velocities. To reduce the amount of data, it is necessary to select typical figures which illustrate salient features of the nature of the velocity dafs. Thus Figure 2(a) shows velocity daf(s) of the forced and free motion versus τ/T for a symmetrical (s=2), N type boom.

Since the greater of the forced and free motion daf(s) is of concern for instantaneous damage, subsequent figures only show the overall maximum velocity daf for each value of τ/T. Graphs (b) through (f) of Figure 2 show the effect of varying the pulse length parameter s and the rise time ratio r_1. Results for displacement dafs for the same system and similar excitations have been obtained by Crocker and Hudson (6) and Cheng and Benveniste(7). The following four main observations can be outlined from Figure 2 (and those not shown here).

(i) The free motion velocity daf is identical to the corresponding displacement daf for any type of sonic boom. For example, the free

motion velocity dafs in Figure 2(a) are equal in magnitude to the corresponding displacement dafs obtained in reference 6.

(ii) When r_1 is increased for a type P boom, the impulse of the boom remains the same - only the shape changes. (Here the 'shape' of the boom is considered to be dependent on the rise time parameters r_1 and r_2 and the duration of the boom between p^+ and p^- (t_p in Figure 1b). If r_2 and t_p change in a similar manner to r_1, the 'shape' is said to be unaltered. However, if either of these behave differently to r_1, the 'shape' is considered to be changed). However, the overall maximum daf which occurs at $\tau/T = 0.5$ (Figure 2(e)) increases with r_1. For type Q and R booms on the other hand, the impulse of the negative pressure phase of the boom increases by 40% when S is increased from 1.6 to 2.2. Note, however, that the shape of the pulse remains unaltered (it is still described by either a sine or cosine function) and the increase in the overall maximum daf is only about 5%. These results suggest that, for a given peak pressure, the overall maximum daf is more dependent on 'shape' than the impulse of the boom.

(iii) The free motion daf is greater (i.e. more critical from a damage standpoint) than that of the forced motion for most values of τ/T considered. Also, all the daf peaks in these figures correspond to free motion dafs.

(iv) The values of τ/T at which the daf peaks occur change due to variations in the sonic booms.

Figure 3 shows the curve which envelopes the maximum velocity dafs for all variations considered previously. But to obtain a

conservative approximation of the maximum possible velocity of the structure (which is of interest from the viewpoint of damage), only the free motion dafs need be determined. (See conclusion (iii) above). Hence an alternative method to that considered previously is presented in Appendix A. The proposed method evaluates the free motion dafs directly in terms of the Fourier Transform of the transient excitation. The Fourier Transform of an actually recorded boom over a full-scale structure can be determined experimentally using a real-time analyzer (details are given in reference 22). Although no actual assessment is made of the saving in computational effort obtained with this method, it is felt that the method should be more efficient than the tedious numerical computations necessary to obtain approximate free motion dafs. This should be true especially in the case of complicated pulses.

A comparison of the maximum velocity dafs in Figure 3 with those of displacement in reference (6) and (7) shows that they are identical for a similar range of variations in the five idealized booms shown in Figure 1(b). (Note, however, that the displacement daf is non-dimensionalized as $\frac{x_{max}}{p^+/m\omega^2}$ whereas the velocity daf is given by $\frac{x_{max}}{p^+/m\omega}$.) Hence, Figure 3 can be used to evaluate maximum displacement dafs.

Measured values of displacement dafs produced by actual sonic boom loadings on vertical studs of houses are shown in Figure 3 (which also gives theoretical values of maximum displacement dafs). These values have been taken from reference (20). It can be seen that the actual dafs lie well below the theoretical daf values given by the envelope

constructed in Figure 3. Hence, it is felt that using this envelope should result in an overestimate of the peak displacements of the wall-like component of the structure.

1.5 Structural Damage Curve

No criterion has been established yet for structural damage caused by sonic booms. However, it is felt reasonable to assume that damage will be like that observed from blasting operations as both disturbances are similar in nature. But a variety of structural damage criteria have been proposed for blasting operations based upon limiting values of displacement, velocity or acceleration.

Edwards and Northwood (4), however, indicate that for a variety of damage mechanisms involving predominant frequencies ranging from 2.5 to 400 Hz, a peak velocity of 4.5 inches per second gives the best correlation with structural damage threshold. The damage threshold is defined here as the opening of old cracks, formation of new plaster cracks or dislodging of loose objects.

In previous sections, the peak velocity of wall-like components caused by typical sonic booms was determined. These results can be used with the proposed damage criterion to give a sonic boom peak pressure, p^+, for which the type of damage indicated above is likely to occur to walls. (The value of p^+ thus obtained, however, is only valid for a boom which is similar in shape to those shown in Figure 1a). Now the velocity daf is given by

$$\text{daf} = \frac{\dot{x}_{max}}{p^+/m\omega} \tag{5}$$

so that, for a damage threshold of 4.5 in/sec,

$$\frac{p^+_{damage}}{m\omega} = \frac{4.5}{daf} \tag{6}$$

where m and ω are the mass and the fundamental circular frequency of the wall respectively. Similarily, for a recommended safe limit of 2 inches per second (23)

$$\frac{p^+_{safe}}{m\omega} = \frac{2.0}{daf} \tag{7}$$

Figure 4 shows simple design curves of $\frac{p^+}{m\omega}$ versus $\frac{\tau}{T}$ for the proposed damage threshold and safe limit criteria. p^+ for likely damage can be determined from these curves once the material properties (m and ω) of wall-like components are known.

1.5.1 A Note on the Discussion of the Application of the Damage Curve to Walls

To use the damage curve, the designer needs to determine the mass per unit area, m, and the fundamental circular frequency, ω, of the wall. The mass per unit area can be computed easily for known material properties. The calculation of ω, on the other hand, is more difficult as the effects of the geometric configuration and edge conditions of the wall have to be considered. A simple approach is suggested next to determine ω for any shaped wall. Before discussing the assumptions involved in this procedure, it is pertinent to consider a few facts regarding the damage curve and sonic booms.

Equation (6) suggests that damage is more likely to occur at smaller values of ω for particular values of m and the daf.

Also, the minimum and most critical value of $\frac{p^+}{m\omega}$ for damage is 1.4 in Figure 4. It occurs when $\frac{\tau}{T} = 0.5$. (or when the duration of the boom matches the natural period of the idealized system). Now the total duration of a sonic boom may vary (22) from about 100 msec for fighter aircrafts to approximately 400 msec for supersonic passenger-transports. Hence τ may vary from approximately 50 msec to 200 msec. This suggests that walls having values of $\frac{\omega}{2\pi}$ ranging from 2 to 10 Hz (i.e. T varies from 500 msec to 100 msec) can have the minimum value of 1.4 for $\frac{p^+}{m\omega}$ corresponding to $\frac{\tau}{T} = 0.5$. Therefore, whenever the wall's estimated natural frequency falls between 2 and 10 Hz, the possibility of damage should be assessed by using the minimum value of $\frac{p^+}{m\omega}$ in order to account for possible variations in the sonic boom's duration.

A procedure is suggested next which should give a useful approximation of ω for non-rectangular walls and walls with openings. When confronted with this situation, the design engineer may:

(i) Idealize the wall as a homogeneous, isotropic linear plate by neglecting the effects of geometrical and structural discontinuities such as columns, sills, doors and windows. For a stud-plaster-board combination wall, the portion of wall between the studs should be considered as an individual plate.

(ii) Determine the net area of the wall by excluding openings such as windows and doors. Take the dimension of the base edge of

the idealized plate, a, identical to the original wall's. Then determine the pseudo height b which, when adjusted, ensures that the product ab equals net area of the original wall.

(iii) Assume simply-supported conditions on all edges. (This should result in a smaller value of ω and, hence, give a conservative estimate of p^{+}_{damage}.)

The approximation of the fundamental frequency of the original wall, ω, can be determined now by using the relationship

$$\omega = \sqrt{\frac{Dg}{\rho_{ST}}} \quad \pi^2 \left(\frac{1}{a^2} + \frac{1}{b^2} \right). \tag{8}$$

D is the flexural rigidity and ρ_{ST} is the surface density of the original wall. An actual single-thickness brick wall of a full-scale structure is considered next in order to investigate the validity of this simple approach. Details of the wall are given in reference (15). The walls (shown in Figure 5) have supporting brick pilasters. The left and right-hand side walls differ in that the former has a door and sill. Base edges of the walls are horizontal but the top edges slope continuously from one vertical edge to the other.

Dimensions and material properties of the walls are:

$a = 17$ ft - 3 in (207 in)

$h = 4.5$ in

$E = 1.5 \times 10^6$ lb/in^2

$\rho_{ST} = 0.2473$ lb/in^2

$\nu = 0.15$

Then $(\text{net area})_1 = 31565 \text{ in}^2$

$(\text{net area})_2 = 33700 \text{ in}^2$

where subscripts 1 and 2 are used to specify left and right-hand side wall, respectively.

Resulting adjusted heights are given by

and,

$$(b)_1 = 31565/207 = 152 \text{ in}$$

$$(b)_2 = 33700/207 = 163 \text{ in}.$$

Using equation (8), it can be shown that

$$(f)_1 = \frac{\omega}{2\pi} = 14 \text{ Hz, and } (f)_2 = 13.4 \text{ Hz}. \qquad (9)$$

The corresponding experimental frequencies of the walls (15) are 17.5 Hz and 23.0 Hz, respectively. This example indicates that the idealization of a wall in the manner suggested should result, for all practical purposes, in a reasonable approximation to the fundamental natural frequency of a brick wall. Also, the effect of a relatively small opening in the wall on the fundamental frequency seems to be negligibly small.

1.5.2 Validity of the Structural Damage Curve

The example of the left hand side brick wall previously considered in section 1.5.1 is examined again to check the validity of the structural damage curve shown in Figure 4. For a typical value of the positive duration of the sonic boom, τ, equal to 100 msec, the value of τ/T equals 1.75. From Figure 4, $\left(\frac{p^+}{m\omega}\right)_{\text{damage}} = 2.0$.

Hence, sonic boom's peak pressure p^+ at which wall damage is likely to occur is given by

$$p^+ = \frac{2.0 \times 0.2473 \times 144.0 \times 17.5 \times 2\pi}{386.4} \quad lb/ft^2$$

or

$$p^+ = 20.3 \ lb/ft^2 \tag{10}$$

The above value agrees generally with damage data reported from actual sonic booms. Reference (25) states that

> 'Other than the 16 day old plaster ceiling, which fell on a 12.1 lb/ft^2 boom, a piece of ceramic tile which fell on 14 lb/ft^2 booms, and glass breakage and very short hairlike extensions and some spalling were observed in old drywall, stucco, and plaster under booms of upto 38 lb/ft^2 in strength'.

It is anticipated that this curve will be a useful guide in assessing the possibility of damage to wall-like components due to sonic boom loading. To establish a safety factor for the structure, however, the effect of pressure doubling which has been neglected in constructing the damage curves (section 1.2) should be incorporated.

1.6 Design Curves for People's Annoyance

Apart from the problem of structural damage, the possibility of people's annoyance as a result of human sensitivity to vibration is of concern. When a sonic boom initially strikes a building, the structure starts vibrating with a severity depending upon the strength of the boom, its incidence and characteristics of the structure. People living in the building may feel the vibration and, consequently, may be irritated or even concerned for the safety of the building.

No reliable information is available at present which shows the effect of short period vibration (of the order of a fraction of a second) on people. Furthermore, no detailed theoretical or experimental studies have been undertaken to determine the response of floors of different types of buildings to sonic boom or similar types of loading. Hence, it is impossible to construct simple design curves with present knowledge which could be used to assess the possibility of people's annoyance created by sonic booms. However, tentative annoyance curves are obtained for people standing on the floor of a tall multi-storey building. The floors are assumed to be supported by steel or reinforced concrete columns. The displacement of a floor of such structures can be approximated simply if the following assumptions are made (26):

(a) The sonic boom is at normal incidence to the span of the vertical structure.

(b) The boom loading is uniform over the front face of the structure.

(c) The floor's response is predominantly in the horizontal direction.

(d) The floor is rigid and the wall columns are attached rigidly at their upper and lower ends to the floors. Then the horizontal displacement of a floor occurs as a result of flexure of the columns which provide the stiffness of the system.

(e) The mass of the walls is small in comparison with the floor.

(f) The structure is cantilevered and its fundamental mode

dominates the displacement.

(g) The effect of the lower floors on the displacement of the top floor which experiences greatest horizontal displacement (and, hence, is the most critical from the viewpoint of people's annoyance) is negligible.

Then the peak displacement of the top floor (see Figure 6a) can be determined in terms of that of an oscillator with mass, m, equal to the mass of the top floor and stiffness k given by (26)

$$k = \frac{12\, n\, E\, I}{l^3} \tag{11}$$

where n = number of columns supporting the floor

E = Young's modulus for column material

I = moment of inertia of column cross-section

l = total height of column.

The total force, F, which acts on the idealized system (see Figure 6b) is given as

$$F(\sigma) = p(\sigma) \times l \times d \tag{12}$$

where $p(\sigma)$ is the pressure-time history of the boom and d is the width of the structure's front face. The fundamental circular frequency of the system is simply

$$\omega = \sqrt{k/m} \tag{13}$$

Then the maximum non-dimensionalized displacement dafs of the floor can be evaluated using Figure 3.

Now Reiher and Meister (5) have obtained annoyance levels of steady state vibrations in terms of peak displacement versus frequency. Intuitively, it is felt that a person will be able to tolerate higher levels of vibration of a transient rather than of a continuous nature.

(This is analogous to the annoyance characteristics of noise). However, the steady state levels are used to determine a tentative criterion for people's annoyance due to short period vibration. The displacement daf of an oscillator is given by

$$daf = \frac{x_{max}}{p^+/m\omega^2} \tag{14}$$

For annoyance, $x_{max} = x_{annoying}$ so that

$$\left(\frac{p^+}{m\omega^2}\right)_{annoying} = \frac{x_{annoying}}{daf} \tag{15}$$

The value of the daf, however, depends upon the frequency of the oscillator and the duration of the sonic boom (Figure 3). Therefore, the design curves are presented in the form $(p^+/m\omega^2)_{annoying}$ versus natural frequency of the idealized system, f, for representative values of τ (Figure 7).

To obtain confidence in the reliability of these curves, research is required to determine:

(i) the response of floors to sonic boom or similar type of loading in various types of structures; and

(ii) an annoyance criterion for short period vibrations typical of boom loadings.

1.7 Conclusions

The peak velocities of wall-like components resulting from typical sonic booms have been obtained using Duhamel's Integral. It has been shown that, for a particular sonic boom, the peak values of non-dimensionalized free motion displacements and velocities of a linear undamped oscillator are identical. Furthermore, it has been found that only the free motion dafs need be determined when constructing overall daf envelope. An alternative method is proposed which evaluates the free motion dafs directly in terms of the Fourier Transform of an excitation, and this can be determined easily using a real-time analyzer. A design curve is obtained for assessing the possibility of damage to wall-like components due to sonic booms. A simple method is suggested and subsequently employed to determine the fundamental frequency, ω, of an actual brick-wall approximately for use with the damage curve. It has been shown that the value of the sonic boom peak pressure, p^+, obtained for a brickwall is in general agreement with damage data reported for actual booms.

Only tentative curves have been obtained for people's annoyance to structural vibrations created by sonic booms. An example of a multi-storey building is considered but no verification of the tentative curve can be made due to the lack of relevant data at present.

PART II

2.0 Introduction

Matrix methods for the dynamic analysis of structures have developed rapidly in recent years. Using one of these methods, the finite element displacement method, a structure may be represented by a number of finite elements. The form of the displacement within an element is usually approximated by a polynomial expression which contains the nodal deflections as unknown constants. These unknowns are determined in such a way that the total energy of the idealization is stationary. However, a realistic idealization of a complex structure often leads to a problem involving such a large number of unknowns that the solution can be very expensive. Furthermore, computer storage requirements become excessive when only a hundred unknowns are used. Thus it would be beneficial to reduce the order of such systems providing results can be obtained which are still sufficiently accurate for practical purposes.

The classical technique (30) is to eliminate those co-ordinates at which no external forces are applied. A technique which gives more accurate natural frequencies than the classical technique (29) is considered here. This technique, proposed initially by Irons (29), is called the elimination technique. It requires only a small proportion of the nodal "deflections" called master deflections to be retained. ("Deflection" in this context means displacements and their spatial derivatives). The remaining "slave" deflections

take values giving least strain energy for the complete system - regardless of the effect they have on the system's total kinetic energy. Reference (31) points out that the suppressed degrees of freedom correspond to high frequencies when satisfactory results are obtained. However, it is possible to suppress or falsify the lower frequencies if inappropriate deflections are eliminated. Furthermore, the usefulness of the technique has been established todate mainly for free vibration problems. In transient vibrations, however, slave deflections create inaccuracies due to deviations not only in the system's total kinetic energy but also in the work done by the external forcing function.

The purpose of this work is twofold. First, to assess further the effect of selecting different master deflections for vibrating systems only considered in a limited fashion previously. Second, to estimate the effect of the elimination technique on a system's transient response by comparison with "exact" results. It should be emphasized at the outset that the primary purpose is to investigate the applicability of the elimination technique rather than the efficiency of computational techniques (such as the frontal (29) or planar storage techniques (28)). Consequently no attempt has been made to optimize computational procedures so that, for example, normal storage (28) is used.

The particular example of a simply-supported, 40:27 rectangular plate in bending is considered because exact solutions are known. Two examples of transient loads are considered - (i) an instantaneous step pressure applied uniformly over the plate;

and (ii) an instantaneous step pressure concentrated at the centre of the plate - as their spatial distributions encompass extremes of structural loading encountered in practical situations. (See Figure 8). For convenience, they are called uniform and point loads, respectively.

2.1 Application of Finite Element Displacement Method to Plate Vibrations

The plate is considered to be perfectly elastic, homogeneous and isotropic. Its transverse displacement is assumed small compared with the wavelength of flexural vibration and stretching of the middle plane of the plate is considered negligible.

The plate is represented by a number of rectangular elements and the displacement distribution $w(x,y,t)$ within an element is approximated by

$$w(x,y,t) = \{w\}_e^T \{f_x f_y\} \tag{16}$$

$\{w\}_e$ is a time-varying vector containing the unknowns; vector $\{f_x f_y\}$ is the product of appropriate distribution functions in the x and y directions (32,33).

Two different forms of the element displacement function are considered. The first form uses the transverse displacement (w), slopes (w_x and w_y) and twist (w_{xy}) as the unknown nodal deflections. The second also includes the curvatures w_{xx} and w_{yy} as unknowns. Then the total number of unknowns for a rectangle is 16 and 24 for the two displacement functions. Hence they are known as the 16 and 24 degree -of-freedom element, respectively. Reference (32), (33) and (34) used the first element in the analysis of plate problems.

Reference (32) also applied the second element to similar problems.

The standard equation of motion with no damping is obtained by using the Euler-Lagrange equation for each element. It takes the form

$$\underline{M}_e \{\ddot{w}\}_e + \underline{K}_e \{w\}_e = \{F\}_e \tag{17}$$

where $\underline{M}_e$ and $\underline{K}_e$ are the mass and stiffness matrices of the element, respectively, and $\{F\}_e$ is the external forcing vector acting on the element. (Note:a dot denotes differentiation with respect to time.) The application of compatibility and equilibrium conditions at the nodal points of the elements gives

$$\underline{M}\{\ddot{w}\} + \underline{K}\{w\} = \{F\} \tag{18}$$

as the equation of motion for the complete plate.

Some of the nodal deflections must be constrained to zero next in order to include the plate's edge conditions. However, only displacement constraints can be applied directly to equation (18). Some disagreement exists in published literature whether higher displacement derivatives corresponding to force boundary conditions should be employed for simply-supported edges (35). Only kinematic conditions are used here. They require the displacement and slope in the edgewise direction to be constrained to zero at all nodal points on the simply-supported edge (28). The constraints necessitate removing appropriate elements from $\{F\}$ and rows and columns from $\underline{M}$ and $\underline{K}$. Then equation (18) is reduced to the form

$$\underline{M}_c\{\ddot{w}\}_c + \underline{K}_c\{w\}_c = \{F\}_c \tag{19}$$

where $\{w\}_c$ contains only the independent, non-zero nodal deflections. The order of the matrices in equation (19) is called the system's constrained degrees of freedom. The above set of second-order differential equations may be solved to evaluate the forced response subject to the conditions

$$\{w(o)\}_c = \{\dot{w}(o)\}_c = \{o\} \tag{20}$$

as the plate is initially at rest.

For free vibrations,

$$\{F\}_c = \{o\} \text{ and } \{\ddot{w}\}_c = -\omega^2\{w\}_c \tag{21}$$

ω is the circular natural frequency. Equation (19) then takes the form

$$[\underline{K}_c - \omega^2 \underline{M}_c]\{w\}_c = \{o\} \tag{22}$$

which, for non-singular M_c, may be reduced to the standard eigenvalue problem

$$[\underline{S}_c - \omega^2 \underline{I}]\{w\}_c = \{o\} \tag{23}$$

where $S_c = \underline{M}_c^{-1} \underline{K}_c$. Also, equation (19) becomes independent of the loading so that both the overall constrained mass and stiffness matrices ($\underline{M}_c$ and $\underline{K}_c$) are identical for free and transient vibration problems. Details of these matrices are given in reference (32). Only the determination of the forcing vector $\{F\}_c$ remains to be described.

The forcing vector $\{F\}_e$ acting on an element of area A_e is found by considering the work done B_e on the element by the external pressure $p(x,y,t)$ in a virtual displacement. Hence,

$$B_e = \int_{Ae} p(x,y,t)\, w(x,y,t)\, dxdy = \{w\}_e^T \{F\}_e. \tag{24}$$

Using equation (16),

$$\{F\}_e = \int_{A_e} p(x,y,t)\{f_x f_y\}\, dxdy. \tag{25}$$

For the two particular loading conditions shown in Figure 8, the forcing function $p(x,y,t)$ has the separable form

$$p(x,y,t) = P(x,y)\, H(t). \tag{26}$$

$H(t)$ is Heavyside's unit step function defined as

$$H(t) = \begin{cases} 0 & t < 0 \\ 1 & t > 0 \end{cases} \tag{27}$$

Now
$$P(x,y) = p_o \tag{28}$$

for a load uniformly distributed over the plate and

$$P(x,y) = p_o\, \delta_x^{x_1}\, \delta_y^{y_1} \tag{29}$$

for a load applied at the point (x_1,y_1) where δ_p^q is given by

$$\delta_p^q = \begin{cases} 0 & p \neq q \\ 1 & p = q \end{cases} \tag{30}$$

Hence, the time invariant vector

$$P(x,y) \int_{A_e} \{f_x f_y\}\, dxdy$$

in equation (25) can be separated from the time dependent part $H(t)$ - simplifying the integration. Details of the generation of the overall constrained vector $\{F\}_c$ are given in reference (16) and (36).

2.2 The Elimination Technique

In the elimination technique proposed by Irons (29) for free vibrations, only a small proportion of the nodal deflections are retained as master deflections. The remaining slave deflections take the values giving least strain energy for the complete system - regardless of the effect these slaves have on the system's total kinetic energy. This technique is employed here primarily for transient vibration problems. A typical process in reducing the size of the problem represented by equation (19) can be outlined as follows (further details being given in reference 29).

The strain energy S.E. of the system can be written as

(31)

$$\text{S.E.} = \frac{1}{2} \{w_1, w_2, \ldots w_s \ldots w_n\}_c \underline{K}_c \begin{Bmatrix} w_1 \\ w_2 \\ \vdots \\ \vdots \\ w_n \end{Bmatrix}_c \qquad (31)$$

If w_s is selected as a slave deflection, the condition that minimizes the strain energy with respect to w_s is obtained by differentiating equation (31) with respect to w_s and equating the result to zero. This gives

$$K_{s1} w_1 + K_{s2} w_2 + \ldots\ldots + K_{ss} w_s + \ldots\ldots + K_{sn} w_n = 0. \qquad (32)$$

Coefficients $K_{s1}, K_{s2} \ldots\ldots K_{sn}$ are constants for a structure whose stiffness is invariant with time. In these cases, differentiating equation (32) with respect to time gives

$$K_{s1} \ddot{w}_1 + K_{s2} \ddot{w}_2 + \ldots\ldots + K_{ss} \ddot{w}_s + \ldots\ldots + K_{sn} \ddot{w}_n = 0. \qquad (33)$$

Substituting for w_s and $\ddot{w}_s$ in equation (19) gives the ij th element of the reduced matrix $\underline{K}^*$ as

$$(K_{ij})^* = K_{ij} - K_{is}\,(K_{js}/K_{ss}). \tag{34}$$

Similarily, $\underline{M}_c$ becomes $\underline{M}^*$ with the ij th element taking the form

$$(M_{ij})^* = M_{ij} - M_{is}(K_{js}/K_{ss}) - M_{js}(K_{is}/K_{ss}) + M_{ss}(K_{is}/K_{ss})\,(K_{js}/K_{ss}). \tag{35}$$

$\{F\}_c$ also becomes $\{F\}^*$ - whose ith element is

$$(F_i)^* = F_i - F_s\,(K_{si}/K_{ss}). \tag{36}$$

Thus for transient vibrations, equation (19) and (20) reduce to

$$M^*\{\ddot{w}\}^* + K^*\{w\}^* = \{F\}^* \tag{37}$$

with initial conditions $\{w(o)\}^* = \{\dot{w}(o)\}^* = \{o\}$. (38)

Equation (23) - the free vibration case - takes the form

$$[\underline{S}^* - \omega^2 I]\{w\}^* = \{o\}, \tag{39}$$

where $\underline{S} = \underline{M}^{*-1}\underline{K}^*$. For convenience the system represented by equations (37) and (39) is called the "reduced" idealization. Its size equals the number of master deflections retained from the initial finite element idealization of the original system.

A computer program has been written which eliminates the selected slave deflections and obtains the required reduced forms of the mass, stiffness and force matrices. It is given in Appendix C.

To investigate further the effect on accuracy of eliminating different deflections, approximate natural frequencies of a simply-supported rectangular plate are obtained from various reduced idealizations and compared with exact values. Subsequently, the effect of the

elimination technique on the plate's transient response due to the loadings shown in Figure 8 is assessed by comparing approximate results with the exact responses.

2.3 Free Response

The elimination technique is applied to a grid containing 16 elements. Two different rectangular elements are used separately. The first one has 16 and the second has 24 degrees of freedom. This results in a total of 64 and 82 constrained degrees of freedom, respectively, for the idealized simply-supported, rectangular plate. The effect of eliminating different deflections is assessed by comparing the accuracy of corresponding computed natural frequencies of free vibrations. Accuracy is determined in terms of the percentage error which is defined as

$$\text{percentage error} = \left(\frac{\text{approximate value-exact value}}{\text{exact value}}\right) \times 100\%. \quad (40)$$

Exact natural frequencies of a simply-supported plate in bending are given by (38)

$$\omega_{mn}^2 = \frac{Dg\pi^4}{\rho_{ST}} (m^2/a^2 + n^2/b^2)^2. \quad (41)$$

ω_{mn} is the circular frequency corresponding to wave numbers (number of half waves) m and n in the x and y directions of the plate, respectively; a and b are the x and y dimensions of the plate. Approximate results are obtained from the solution of the eigenvalue problem (39). Using double precision arithmetic, the solution is obtained numerically by using Householder's method of reducing $\underline{S}^*$ to an upper Hessenberg matrix and applying the QR double-step algorithm. Details of this method are given in reference (37). The lowest natural frequencies of various

reduced idealizations are presented in Tables 2 and 3. The largest computed frequencies are also given but in the non-dimensionalized form

$$\frac{(\mu_{max})_{KS}}{(\mu_{max})_{KS_{max}}} \tag{42}$$

KS and KS_{max} are the degrees of freedom of the reduced and original idealization, respectively. (The reason for considering the greatest frequency is because it can cause numerical instability in the direct integration of the transient equations of motion considered in the next section.) Results obtained by Mason (32) with fewer elements are also given in Tables 2 and 3as a basis of assessing the usefulness of the elimination technique. A flow diagram and brief description of the computer programs used to solve the eigenvalue problem are given in Appendix C.

To determine approximately the relative computational time involved in solving the eigenvalue problem, computer times required for an IBM 360-65 digital computer are listed in Table 4 for the largest problems considered. It can be seen that the computer time (C.P.U. time) is approximately proportional to $KS^{2.5}$ where KS is the size of the eigenvalue problem. This indicates that significant savings can be made for even small reductions in the size of large problems.

A comparison of Tables 2 and 3indicates that the original idealizations (case A1 and B1) always give the most accurate lowest frequencies. However, these tables also show that the percentage error in the fundamental frequency is small but four to five times that of the original idealization when displacements alone are retained at all interior nodal points (case A6 and B6). Although the 16 degrees-of-freedom element produces comparable ratios for the four lowest modes the element with 24 degree -of-freedom may give significantly higher

values. Retaining slopes in addition to the w's at the same nodes (case A5 and B5) increases the size of the problem by three times. The decrease in corresponding errors is marginal for the first few modes, becoming more reasonable for the higher modes. Keeping second derivatives too as in case A4 and B4 raises the size by four and six times that of A6 and B6, respectively. The increase in accuracy obtained by including the twist, w_{xy}, is small when using the 16 degree -of-freedom element. Fair improvement is obtained for all frequencies when the curvature terms, w_{xx} and w_{yy}, of the 24 degree -of-freedom element are included as master deflections. Similar trends occur when the five interior points shown in case A7, A8, A9, B7, B8 and B9 are considered. Consequently these results also indicate that the accuracy of the lowest natural frequencies generally improves as the number of master variables at a given set of nodal points is increased. The displacement, however, appears to be the single most important variable at a nodal point. Therefore, for a given problem size, it could be advantageous to retain displacement at a larger number of points to the exclusion of derivatives. For example, retaining displacements at all interior nodes (A6 and B6) usually produces lower errors and results in a smaller problem than keeping all the variables at fewer points (A7 and B7). Similar results not shown in these tables were obtained involving fewer master deflections. Also, even in the extreme case when the displacement alone is retained at the central node and (case A11 and B11) the percentage error of the fundamental frequency is only 6 to 8%. Although this last suggestion may only be valid for problems which do not have strong localized displacements (31), it is consistent with the more general proposals made by Irons for cantilever-like structures (29).

Irons also points out that displacements near encastered roots should tend to be slaves. The proposal may be extended intuitively to include any point having least flexibility as it will contribute "little kinetic energy in the lower modes" (29). This extension is upheld by the results for the simply-supported plate. For example, it can be seen by comparing case A9 with A10 and B9 with B10 that if the first four modes are important those nodal points having least flexibility (such as points closest to the corners of the supported edges) should preferably be eliminated first.

Although the results for the simply-supported plate further substantiate the usefulness of the elimination technique, an interesting aspect not previously reported is observed. It occurs when the 24 degree -of-freedom element is used to idealize the plate. Table 3 shows that the natural frequencies computed with coarse grids are more accurate than those from a finer grid which employ the elimination technique to reduce the number of degrees of freedom to a comparable value. For example, case B3 produces frequencies which are more accurate than those of case B5 and B6. Furthermore, apart from the first and second frequency, the results of case B3 are more accurate than those of B4. Table 2 shows that this is not the situation with the 16 degrees-of-freedom element. However, no investigation is made here to determine the cause of this difference.

2.4 Transient Response

Equation (37) may be solved by using either normal modes of the freely vibrating system (36) or with a step-by-step numerical integration technique (39). Noting again that the purpose of this work is to investigate the elimination technique rather than the computational efficiency of available techniques, no assessment of the different methods of solving equation (37) is made here. Reference (39) however does discuss the relative merits and demerits of these methods.

A standard fourth order Runge-Kutta procedure is used to solve equation (37) with initial conditions (38) to give the plate's displacement velocity and acceleration at any of the nodal points. For the application of this method, details of which are given in reference (39), a more suitable form of equation (37) is

$$\{\ddot{w}\}^* = -\underline{M}^{*-1}\,\underline{K}^*\{w\}^* + \underline{M}^{*-1}\{F\}^*, \qquad (43)$$

matrix $\underline{M}^*$ being non-singular. The flow diagram and brief description of the computer programs used to determine the transient response from equation (43) are given in Appendix C.

Like all step-by-step integration techniques, the Runge-Kutta method suffers from the conflicting requirements of accuracy and computational effort. A smaller time increment, h, gives more accurate results but requires greater computational effort. Classical theory stipulates that the maximum allowable value of h must satisfy the inequality (39)

$$h < 2.8/\mu_{max} \qquad (44)$$

where μ_{max} is the greatest eigenvalue of the free vibration problem. But this criterion guarantees only that a solution does not diverge; it does not necessarily guarantee an adequate approximation. The most

favoured method of checking accuracy is to repeat the computation with half the time increment and to compare the two sets of results.

The results are regarded as "accurate" if the difference between the two sets is "small". Whether some "small" difference is acceptable can only be based on an engineering assessment of the errors involved in the mathematical idealization of the actual system.

Details of the theoretical analysis for determining the response of a simply-supported rectangular plate to a transverse transient force are given in reference 40. However, the principal equations involved are outlined in Appendix B. The method employs normal modes and its accuracy depends upon the number of modes considered in the computation. Convergence is again checked by comparing the results calculated with two different number of modes being compared. If the difference between the two sets is "small", the results are regarded as "exact". A brief description and listing of the computer program used to compute the "exact" results are given in Appendix C.

2.4.1 Discussion of Results

The particular example of the simply-supported plate shown in Figure 8 is considered here. This plate is subjected to two types of transient loads - (i) an instantaneous step pressure distributed uniformly over the complete plate and (ii) a load having a similar pressure-time history but which is concentrated at the centre of the plate (a point load as indicated in Figure 8). For convenience, they are called a uniform and a point load, respectively. "Exact" and approximate time-histories of displacement, velocity and acceleration at the plate's

centre are evaluated for both types of loading. The approximate results are computed with various systems obtained by eliminating different variables from the 64 constrained degrees-of-freedom idealization given as A1 in Table 2. The response-time histories, however, are presented in non-dimensionalized form. Thus the displacement and velocity are non-dimensionalized as in section 1.3 and the acceleration is divided by p_o/m where p_o is the pressure amplitude and m is the mass per unit area of the plate. Similarly time, t, is divided by the exact fundamental period of the plate, T.

Figures 9 and 10 show the exact and approximate response at the centre of the plate due to the uniform and point load, respectively. The approximate results were evaluated with a step size of $1.0/\mu_{max}$. The effect of using twice and half this step size is also indicated in these figures by the maximum percentage error in the largest positive or negative values of the response variables. The percentage error is given by equation (40) - approximate values being computed with the three step sizes. The exact response-time histories are computed for both types of loads with 200 normal modes of the plate. For the point load, however, exact accelerations could not be established as they do not converge even when this large number of modes is used (27,40).

Figures 9 and 10 show that the main difference between the point and uniform loads is that the former excites high frequency modes more efficiently. However, both "exact" accelerations are seen to be most sensitive to these modes. "Exact" is a misnomer in the case of the acceleration produced by the point load because of the lack of convergence even with 200 normal modes. Hence it is unreasonable to expect the original idealization - which only involves 64 degrees of freedom -

and subsequent reduced idealizations to produce accurate accelerations. Although no such problem exists for the uniform load, the maximum percentage error in the peak acceleration is still about 10% even for the original idealization. As the elimination technique preserves the accuracy of only the lowest modes, acceleration being sensitive to high frequencies is most susceptible to reductions in the original idealization's number of degrees of freedom. Consequently the technique may produce unreliable accelerations. The velocity and displacement on the other hand are usually less sensitive to high frequency modes being affected primarily by the fundamental. Thus the technique can give reasonable displacements and velocities with few degrees of freedom.

Actual savings in computational effort depend partly upon the method of solution and partly upon the efficiency of computation and type of computer facilities available. No attempt is made to investigate the efficiency of available techniques of solution. Also, little effort was made to optimize computational procedures. However, to get a feeling for the saving, computer times required for the solution of the transient problems are given in Table 4. When the Runge-Kutta method is employed, computer time depends not only upon the size of problem (KS) but also upon the step size, h, required for integration. Intuitively the larger is KS and the smaller h, then the greater will be the computational time and effort. However, h is inversely proportional to the highest eigenvalue of the idealized system, μ_{max}, for stability. The results in Table 4 indicate that the computer time is, in fact, approximately proportional to the product $(KS)^2/h$ or $\mu_{max}(KS)^2$. Thus

the saving in computer time can be twofold when using the elimination technique. Firstly KS becomes smaller and, secondly, μ_{max} decreases when satisfactory results are obtained (31). Also, as the time depends upon the square of KS, significant savings can be achieved with even small reductions in the size of large problems. Furthermore if similar accuracies can be obtained by reducing KS and h in about the same ratio than the idealization with the lower values is preferred as computer time will be less. At first sight this conclusion may be surprising in view of the popular impression that reducing the step size necessarily leads to increased computational time. It is true only when KS remains constant as in the classical finite element approach to transient problems. It need not necessarily be the case with the elimination technique where KS is a variable in addition to h.

There are generally two types of error involved in the analysis of a physical system. The first type occurs in the mathematical idealization of the system and the second results from computational errors in the solution process. But the decision whether the computational errors are acceptable can only be based upon an engineering assessment of the idealization errors. For example, it is pointless to use an extremely accurate computational procedure if the original idealization is not sophisticated. But the primary concern here is merely to compare the magnitude of the errors introduced by the elimination technique with the total error produced by an original, unreduced idealization. Errors from the technique are deemed "acceptable" if they are comparable at worst to the total error of the original idealization. They are evaluated by assessing the difference in the transient response before

and after applying the elimination technique.

It has been seen that the accuracy and, hence, acceptability of results depends not only upon the number of modes excited by the load but also upon whether they contribute significantly to the different response parameters. Thus, although free vibration characteristics evaluated using the elimination technique will give some indication of the accuracy of transient cases, intuitive judgement is still needed. Factors which should be taken into consideration include the type of load, the main response parameters of interest and the positions at which they are to be evaluated.

Optimum combinations of step and problem size which minimize computational time and effort but still give acceptable results for loads encompassing extremes of spatial distribution are indicated in Table 5 for the reductions considered. Three response parameters - the displacement, velocity and acceleration - are appraised. Table 5 shows that the step size parameter, $\mu_{max}h$, should have a value of one at most for optimum conditions. This value agrees with that proposed by Craggs (27) for "adequate" results with conventional procedures. It can also be seen from Figure 9 and 10 that reduced idealizations having five or more degrees of freedom can give acceptable results for those response parameters affected by higher modes - providing, of course, no convergence difficulty exists. Thus, of the cases considered for these parameters, KS has an optimum value of five (Table 5).

It should be remembered that antisymmetric mode shapes in both directions are not excited by either the point or uniformly distributed load as might be the situation, for example, with a wave travelling

over the plate (16). (Even if these modes had been excited, they would be effective only at points away from the centre of the plate - hence, the importance of position.) Therefore it is quite possible that more than five degrees of freedom may be required for acceptable results if anti-symmetric modes contribute significantly to response parameters at points of interest. If, on the other hand, a parameter is dominated by the fundamental mode (e.g. the exact displacements in Figure 9 and 10) then acceptable approximations can be produced with an optimum KS size of unity as indicated in Table 5.

2.5 Conclusions

The elimination technique has been employed to reduce the number of variables idealizing a simply-supported, rectangular plate. It is found that the computer time required for the solution of large free vibration problems is approximately proportional to $KS^{2.5}$ - suggesting that significant savings in computational effort can be made with even a small reduction in size, KS. As regards accuracy, the original (unreduced) finite element idealization is seen to give the most accurate natural frequencies. Also, the accuracy of the lowest frequencies generally improves as the number of master variables at a given set of nodal points is increased. The displacement, however, appears to be the single most important variable at a nodal point. Therefore, for a given problem size, it could be advantageous to retain displacements at a larger number of points to the exclusion of derivatives. But it should also be remembered that variables (including displacements) at nodal points closest to the corners of the supported edges should preferably

be among the first to be eliminated. These last two suggestions agree with the more general proposals made by Irons for cantilever-like structures. An interesting aspect not previously reported has also been observed. It has been demonstrated that using fewer 24 degrees-of-freedom elements to decrease the size of the eigenvalue problem results in more accurate natural frequencies than those obtained from reduced idealizations of comparable size.

Accelerations which are sensitive to high frequencies are most susceptible to reductions in the original idealization's number of degrees of freedom. Consequently, the elimination technique may produce unreliable accelerations. The technique, however, can give reasonable displacements and velocities with few degrees of freedom. It is found that the computer time required for the solution of large transient vibration problems is approximately proportional to KS^2/h or $\mu_{max}(KS)^2$. This leads to the suggestion that when similar accuracies can be obtained by reducing KS and h in about the same ratio, the idealization with lower values should be preferred in order to save computational time and effort. At first sight this conclusion contradicts the popular impression that reducing the step size necessarily leads to increased computational time. It is only true when KS is constant as in the conventional finite element approach to transient problems.

It has been shown that the step size parameter, $\mu_{max}h$, should have a value of one at most for adequate results. Furthermore, the reduced idealizations having five or more degrees of freedom are seen to give acceptable results for those response parameters affected by higher modes - providing no convergence difficulty exists. Thus,

of the cases considered, KS has an optimum value of five. It is pointed out, however, that more than five degrees of freedom may be required if antisymmetric modes contribute significantly to response parameters at points of interest. If, on the other hand, a parameter is dominated by the fundamental mode then acceptable approximations can be produced with an optimum KS value of unity.

REFERENCES

1. G.B. Whitham — The flow pattern of a supersonic projectile. Comm. Pure and Applied Math. 5:301. 1952.

2. H.H. Hubbard, D.J. Maglieri, V. Huckel — Ground measurements of sonic boom pressures for the altitude range of 10,000 to 75,000 feet. NASA TR R-198. 1964.

3. D.A. Hilton, V. Huckel, R. Steiner, D.J. Maglieri — Sonic boom exposure during FAA community-response studies over a 6-month period in the Oklahoma City area. NASA TN D-2539. 1964.

4. A.T. Edwards, T.D. Northwood — Experimental studies of the effects of blasting on structures. The Engineer, 538-546. 1960.

5. H.J. Reiher, F.J. Meister — Human sensitivity to vibration. 1931. Forsch. auf dem Geb. des. Ing., 2, 11, 381-6. (Transl. Rep. F-TS-616-RE, Wright Field, 1946).

6. M.J. Crocker, R.R. Hudson — Structural response to sonic booms. J. Sound Vib. 9(3), 454-468, 1969.

7. D.H. Cheng, J.E. Benveniste — Sonic boom effects on structures - a simplified approach. Trans. of the New York Academy of Sciences, Series II, Vol. 30, No. 3, 457-478, Jan. 1968.

8. ARDE Associates — Response of structures to aircraft generated shock waves. WADC U.S. Air Force Tech. Rept. 58-169. 1959.

9. M.J. Crocker, R.R. Hudson — Response of a simple system to a sonic boom. University of Liverpool, Dept. of Building Science, Rept. BS/A/68. 1968.

10. J.E. Benveniste, D.H. Cheng — Transient response of structural elements to travelling pressure waves of arbitrary shape. Int. J. Mech. Sci. 8, 607. 1966.

11. M.J. Crocker — Multimode response of panels to normal and to travelling sonic booms. JASA 42,5. 1967.

12. D.H. Cheng — Dynamic response of structural elements to travelling 'N' shaped pressure waves. NASA LWP 147. 1965.

13. A, Craggs — The response of a simply-supported plate to transient forces, Part II - The effect of N-waves at oblique incidence. NASA CR-1176. 1968.

14. N, Popplewell — The vibration of a box-type structure (II): response to a travelling pressure wave. J. Sound Vib. 18(4), 521-531, 1971.

15. N, Popplewell — Finite element idealizations of a full-scale building. Presented at the British Acoustical Society meeting "Finite element techniques in structural vibration", March 1971.

16. N. Popplewell — Response of box-type structures to sonic booms. Ph.D. Thesis presented to the University of Southampton, 1969.

17. C.H.E. Warren — A significant single quantity that typifies sonic bang. RAE Structures Dept. Note, Jan. 1970.

18. W. Bleakney, D.R. White, W.C. Griffith — Measurements of diffraction of shock waves and resulting loading of structure. J. App. Mechanics 17, 439-455, 1950.

19. J.K. Wright — Shock Tubes. London: Methuen. 1961.

20. B.L. Clarkson, W.H. Mayes — Sonic boom induced building structure responses including damage (University of Southampton). Presented at an ASA meeting.

21. W.T. Thomson — Vibration Theory and Applications. N.J., Prentice-Hall. 1965.

22. — — B & K Technical Review No. 1, 1970.

23. W.I. Duvall, D.E. Fogelson — Review of criteria for estimating damage to residences from blasting vibrations.

24. S.P. Timoshenko, S. Woinowsky Kreiger — Theory of Plates and Shells, New York, McGraw-Hall, 2nd edition, 1959.

25. J.H. Wiggins — The effects of sonic boom on structural behaviour. A.R.C. 29.112 N522. May 1967.

26. C.E. Crede — Shock and Vibration Concepts in Engineering Design. Prentice-Hall, N.J. 1965.

27. A. Craggs — The response of acousto-mechanical systems to sonic booms. Ph.D. Thesis presented to the University of Southampton, 1968.

28. V. Mason — The effect of acoustic radiation on the vibration response of plane structure. Ph.D. Thesis, University of Southampton. 1968.

29. B.M. Irons — Structural eigenvalue problems - elimination of unwanted variables. AIAA Jul 3, 961 (1965).

30. R.J. Guyan — Reduction of stiffness and mass matrices. AIAA Jnl 3, 380. 1965.

31. R.G. Anderson, B.M. Irons, O.C. Zienkiewicz — Vibration of stability of plates using finite elements. Int. J. Solids Structures, Vol. 4, pp. 1031-1055. 1968.

32. V. Mason — Rectangular finite elements for analysis of plate vibrations. J. Sound Vib. 7, 437-448. 1968.

33. F.K. Bogner, F.L. Fox, L.A. Schmit Jr. — Matrix methods in structural mechanics. Wright-Patterson Air Force Base, Dayton, Ohio AFFDL-TR-66-80. The generation of interelement compatible stiffness and mass matrices by the use of interpolation formulas. 1966.

34. G.A. Butlin, F.A. Leckie — Syposium on the numerical methods for vibration problems, University of Southampton. A study of finite elements applied to plate flexure. 1966.

35. N. Popplewell
D. McDonald
Conforming rectangular and triangular plate-bending elements. J. of Sound and Vib. Vol. 19, No. 3, 333-347, 1971.

36. W.C. Hurty
M.F. Rubinstein
Dynamics of structures. New Jersey. Prentice-Hall, 1964.

37. J.H. Wilkinson
The Algebraic Eigenvalue Problem. Oxford: Clarendon Press. 1965.

38. S.P. Timoshenko
S. Woinowsky-Kreiger
Theory of plates and shells, New York, McGraw-Hill, 2nd edition, 1959.

39. F.B. Hilderbrand
Introduction to Numerical Analysis. New York: McGraw-Hill, 1956.

40. G.B. Warburton
The Dynamical Behaviour of Structures. Pergamon Press, 1964.

Type of boom (see Fig. 1b)	Mathematical description of idealized boom	Non-dimensionalized velocity $\dot{x}_n(t) \equiv \dot{x}(t)/\omega x_s$	Time regime
N	$p(\sigma)=p^+(1-\frac{\sigma}{\tau})$	$\dot{x}_n(t)=-\frac{1}{\omega\tau}+\sin\omega t+\frac{1}{\omega\tau}\cos\omega t$	$0\leq t\leq s\tau$
	$p(\sigma)=0$	$\dot{x}_n(t)=(s-1)\sin\omega(t-s\tau)+\sin\omega t+\frac{1}{\omega\tau}\cos\omega t-\frac{1}{\omega\tau}\cos\omega(t-s\tau)$	$t>s\tau$
P	$p(\sigma)=\frac{p+\sigma}{r_1\tau}$	$\dot{x}_n(t)=\frac{1}{r_1\omega\tau}(1-\cos\omega t)$	$0\leq t\leq r_1\tau$
	$p(\sigma)=\frac{p^+}{1-r_1}(1-\frac{\sigma}{\tau})$	$\dot{x}_n(t)=\frac{1}{1-r_1}(\frac{1}{r_1\omega\tau}\cos\omega(t-r_1\tau)-\frac{1-r_1}{r_1\omega\tau}\cos\omega t-\frac{1}{\omega\tau})$	$r_1\tau\leq t\leq(s\tau-r_2\tau)$
	$p(\sigma)=\frac{p^+}{r_2\tau}(\frac{1+r_2-s}{1-r_1})(s\tau-\sigma)$	$\dot{x}_n(t)=\frac{1}{1-r_1}(-\frac{1-r_1}{r_1\omega\tau}\cos\omega t+\frac{1}{r_1\omega\tau}\cos\omega(t-r_1\tau)+\frac{1-s}{r_2\omega\tau}\cos\omega(t-s+r_2\tau)-\frac{1+r_2-s}{r_2\omega\tau})$	$(s\tau-r_2\tau)\leq t\leq s\tau$
	$p(\sigma)=0$	$\dot{x}_n(t)=\frac{1}{1-r_1}(-\frac{1-r_1}{r_1\omega\tau}\cos\omega t+\frac{1}{r_1\omega\tau}\cos\omega(t-r_1\tau)+\frac{1-s}{r_2\omega\tau}\cos\omega(t-s\tau+r_2\tau)-\frac{1+r_2-s}{r_2\omega\tau}\cos\omega(t-s\tau))$	$t>s\tau$
Q	$p(\sigma)=p^+\sin\omega_1\sigma$ $\omega_1=\pi/\tau$	$\dot{x}_n(t)=\frac{\omega_1/\omega}{1-(\frac{\omega_1}{\omega})^2}(\cos\omega_1 t-\cos\omega t)$	$0\leq t\leq\tau$
	$p(\sigma)=-p^+\alpha\sin\omega_2(t-\sigma)$ $\omega_2=\frac{\pi}{(s-1)\tau}$, $\alpha=p^-/p^+$	$\dot{x}_n(t)=-\frac{\omega_1/\omega}{1-(\frac{\omega_1}{\omega})^2}(\cos\omega t+\cos\omega(t-\tau))-\frac{\alpha\omega_2/\omega}{1-(\frac{\omega_2}{\omega})^2}(\cos\omega_2(t-\tau)-\cos\omega(t-\tau))$	$\tau\leq t\leq s\tau$
	$p(\sigma)=0$	$\dot{x}_n(t)=-\frac{\omega_1/\omega}{1-(\frac{\omega_1}{\omega})^2}(\cos\omega t+\cos\omega(t-\tau))+\frac{\alpha\omega_2/\omega}{1-(\frac{\omega_2}{\omega})^2}(\cos\omega(t-\tau)+\cos\omega(t-s\tau))$	$t>s\tau$
R	$p(\sigma)=p^+\cos\omega_1\sigma$ $\omega_1=\pi/2\tau$	$\dot{x}_n(t)=\frac{1}{1-(\frac{\omega_1}{\omega})^2}(-\frac{\omega_1}{\omega}\sin\omega_1 t+\sin\omega t)$	$0\leq t\leq\tau$
	$p(\sigma)=-p^+\alpha\sin\omega_2(t-\tau)$ $\omega_2=\frac{\pi}{2(s-1)\tau}$, $\alpha=p^-/p^+$	$\dot{x}_n(t)=\frac{1}{1-(\frac{\omega_1}{\omega})^2}(\sin\omega t-\frac{\omega_1}{\omega}\cos\omega(t-\tau))-\frac{\alpha\omega_2/\omega}{1-(\frac{\omega_2}{\omega})^2}(\cos\omega_2(t-\tau)-\cos\omega(t-\tau))$	$\tau\leq t\leq s\tau$
	$p(\sigma)=0$	$\dot{x}_n(t)=\frac{1}{1-(\frac{\omega_1}{\omega})^2}(\sin\omega t-\frac{\omega_1}{\omega}\cos\omega(t-\tau))+\frac{\alpha}{1-(\frac{\omega_2}{\omega})^2}(\sin\omega(t-\tau)+\frac{\omega_2}{\omega}\cos\omega(t-\tau))$	$t>s\tau$
T	$p(\sigma)=p^+(1-\frac{1-\alpha+\alpha\beta}{\beta\tau})$	$\dot{x}_n(t)=-\frac{1-\alpha+\alpha\beta}{\beta\omega\tau}+\sin\omega t+\frac{1-\alpha+\alpha\beta}{\beta\omega\tau}\cos\omega t$	$0\leq t\leq\beta\tau$
	$p(\sigma)=p^+\alpha(1-\frac{\sigma}{\tau})$	$\dot{x}_n(t)=-\frac{\alpha}{\omega\tau}+\frac{1-\alpha+\alpha\beta}{\beta\omega\tau}\cos\omega t+\sin\omega t-\frac{1-\alpha}{\beta\omega\tau}\cos\omega(t-\beta\tau)$	$\beta\tau\leq t\leq s\tau$
	$p(\sigma)=p^+\lambda(1-\frac{\sigma-s\tau}{\gamma\tau})$	$\dot{x}_n(t)=-(1-s-\frac{\lambda}{\alpha})\alpha\sin\omega(t-s\tau)+\frac{1-\alpha+\alpha\beta}{\beta\omega\tau}\cos\omega t+\sin\omega t-\frac{1-\alpha}{\beta\omega\tau}\cos\omega(t-\beta\tau)+\frac{\lambda-\alpha\gamma}{\gamma\omega\tau}\cos\omega(t-s\tau)-\frac{\lambda}{\gamma\omega\tau}$	$s\tau\leq t\leq(s\tau+\gamma\tau)$
	$p(\sigma)=0$	$\dot{x}_n(t)=-(1-s-\frac{\lambda}{\alpha})\alpha\sin\omega(t-s\tau)+\frac{1-\alpha+\alpha\beta}{\beta\omega\tau}\cos\omega t+\sin\omega t-\frac{1-\alpha}{\beta\omega\tau}\cos\omega(t-\beta\tau)+\frac{\lambda-\alpha\gamma}{\gamma\omega\tau}\cos\omega(t-s\tau)-\frac{\lambda}{\gamma\omega\tau}\cos\omega(t-s\tau-\gamma\tau)$	$t>(s\tau+\lambda\tau)$

Table 1. Showing the equations of motion of an undamped, linear oscillator subjected to idealized sonic booms.

Case	Procedure	Degrees of freedom, KS	Percentage error						$(\mu_{max})_{KS}/(\mu_{max})_{64}$
			1	2	3	4	5	6	
A1	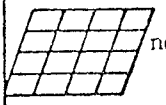 no elimination	64	0.015	0.170	0.320	1.230	0.240	0.650	1.00
A2	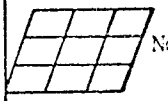 No elimination	36	0.040	0.540	0.960	7.430	0.740	3.560	0.56
A3	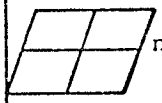 no elimination	16	0.24	5.060	9.060	16.900	6.940	10.900	0.25
A4	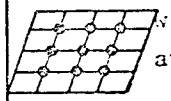 w,w_x,w_y,w_{xy} retained at ringed nodes	36	0.050	0.557	0.727	3.170	1.710	4.770	0.84
A5	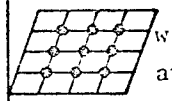 w,w_x,w_y retained at ringed nodes	27	0.050	0.561	0.738	3.205	1.780	4.991	0.59
A6	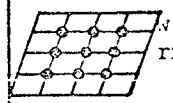 w retained at ringed nodes	9	0.070	0.940	1.130	6.530	3.430	9.850	0.14
A7	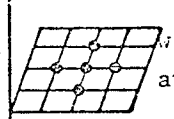 w,w_x,w_y,w_{xy} retained at ringed nodes	20	0.596	0.010	9.060	9.070	38.720	31.400	0.75
A8	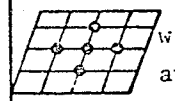 w,w_x,w_y retained at ringed nodes	15	0.596	4.010	9.160	9.070	42.650	31.420	0.58
A9	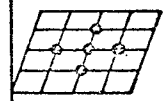 w retained at ringed nodes	5	0.601	5.130	13.830	11.660	101.750		0.10
A10	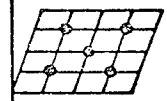 w retained at ringed nodes	5	1.140	5.130	13.830	16.315	3.434		0.05
A11	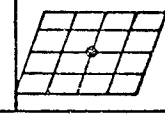 w retained at ringed node	1	6.720						0.01

Constraints applied at nodal points on edges parallel to:

(i) x axis $w = w_x = 0$;

and (ii) y axis $w = w_y = 0$.

Table 2. Showing the percentage errors in the lowest natural frequencies of a 40:27 simply-supported plate using the 16 degrees-of-freedom rectangular element.

Case	Procedure	Degrees of freedom, KS	Percentage error						$(\mu_{max})_{KS}$ / $(\mu_{max})_{82}$
			1	2	3	4	5	6	
B1	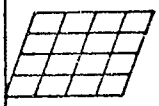 no elimination	82	0.114	0.225	0.104	0.217	0.401	0.682	1.00
B2	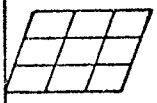 no elimination	44	0.197	0.370	0.167	0.454	0.700	1.786	0.52
B3	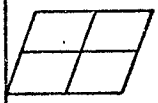 no elimination	18	0.401	1.140	0.200	1.946	0.048	3.200	0.19
B4	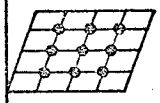 $w, w_x, w_y, w_{xx}, w_{xy}, w_{yy}$ retained at ringed nodes	54	0.148	0.591	0.478	2.171	1.749	4.610	0.95
B5	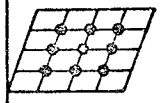 w, w_x, w_y retained at ringed nodes	27	0.439	1.525	2.455	3.980	4.756	8.414	0.38
B6	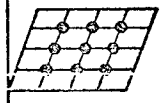 w retained at ringed nodes	9	0.473	2.057	3.290	8.498	6.845	14.260	0.11
B7	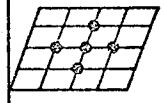 $w, w_x, w_y, w_{xx}, w_{xy}, w_{yy}$ retained at ringed nodes	30	0.560	3.270	7.000	7.160	28.663	17.591	0.90
B8	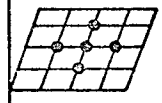 w, w_x, w_y retained at ringed nodes	15	1.040	4.956	9.220	10.284	30.121	17.868	0.36
B9	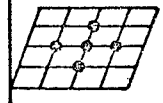 w retained at ringed nodes	5	1.048	6.697	16.442	14.224	112.155		0.08
B10	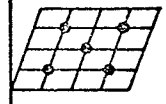 w retained at ringed nodes	5	1.611	6.697	16.442	19.837	6.845		0.04
B11	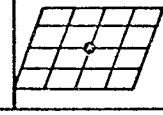 w retained at ringed node	1	7.436						0.01

Constraints applied at nodal points on edges parallel to:

(i) x axis $\quad w = w_x = w_{xx} = w_{yy} = 0;$

and (ii) y axis $\quad w = w_y = w_{xx} = w_{yy} = 0.$

Table 3. Showing the percentage errors in the lowest natural frequencies of a 40:27 simply-supported plate using the 24 degrees-of-freedom rectangular element

Free vibration				Transient vibration				
Case (See Table 2 and 3)	Degrees of freedom, KS	C.P.U. time, τ_F (minutes)	$\frac{KS^{2.5}}{\tau_F}$	Case (See Table 2)	Degrees of freedom, KS	$\mu = \frac{(\mu_{max})_{KS}}{(\mu_{max})_{64}}$	C.P.U. time, τ_T (minutes)	$\mu KS^2/\tau_T$
B1	82	5.42	11200	A1	64	1.00	26.00	1575
A1	64	2.70	12100	A4	36	0.84	7.36	1480
B2	44	1.06	12100	A5	27	0.59	2.70	1590
A2	36	0.65	12000	A6	9	0.14	0.09	1260
B3	18	0.25	5500					
A3	16	0.22	4700					

Table 4. Showing computer times required for the solution of free and transient problems with different values of KS.

	Type of Load					
	Uniformly distributed pressure			Point load		
Non-dimensionalized response	Case	Degrees of freedom, KS	Step size parameter* $\mu_{max}h$	Case	Degrees of freedom, KS	Step size parameter* $\mu_{max}h$
Displacement parameter $w/(p_o/m\omega^2)$	All	1	1.0	All	1	1.0
Velocity parameter $w/(p_o/m\omega)$	All	1	0.5	A6	5	1.0
Acceleration parameter $w/(p_o/m)$	A6	5	0.5		UNACCEPTABLE	

* Note that μ_{max} changes with a reduction in KS (see Table 2).

Table 5. Showing optimum combinations of step and reduced problem size which minimize computational time and give acceptable response characteristics.

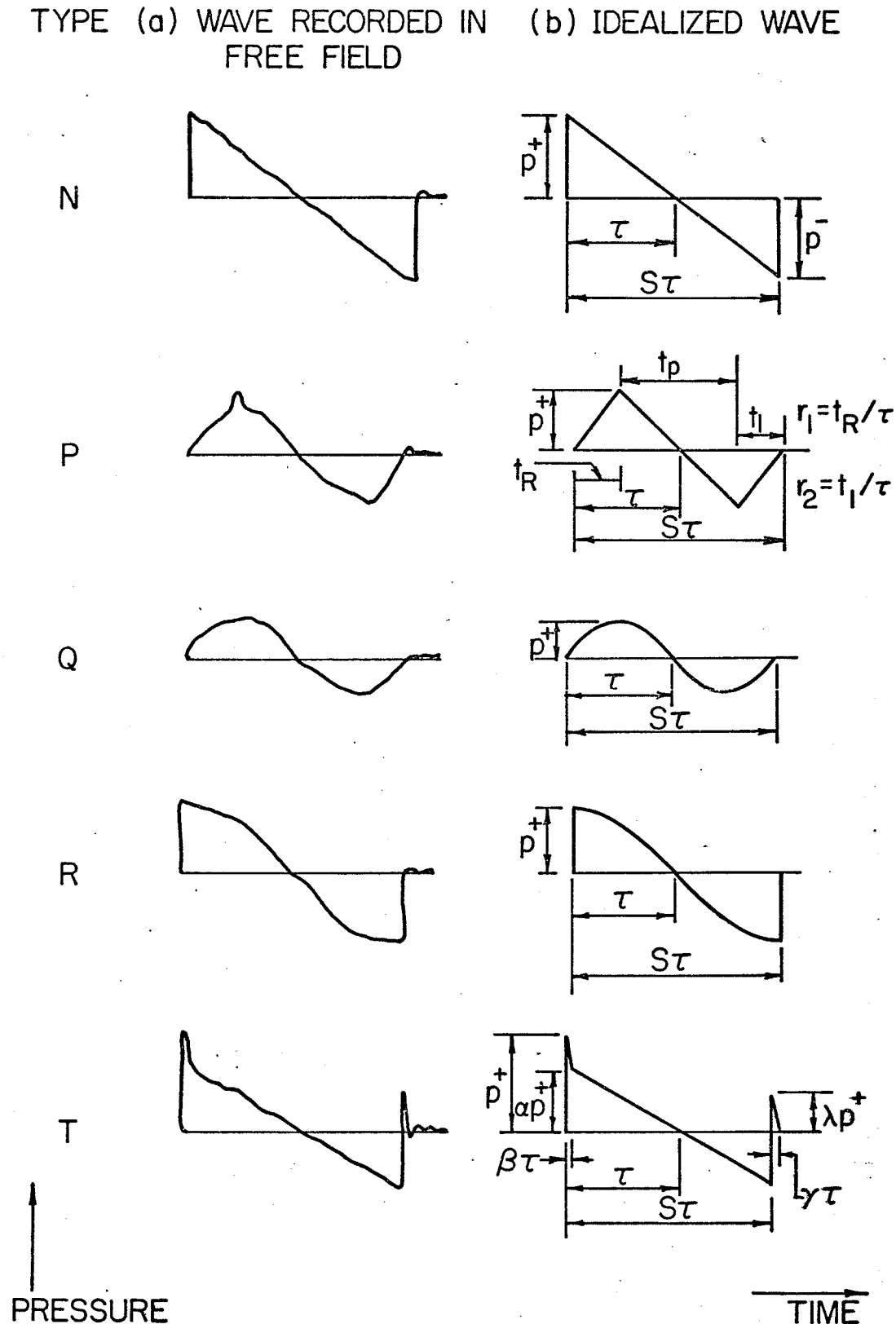

Figure 1. Showing (a) typical waves recorded in free-field and (b) their idealizations

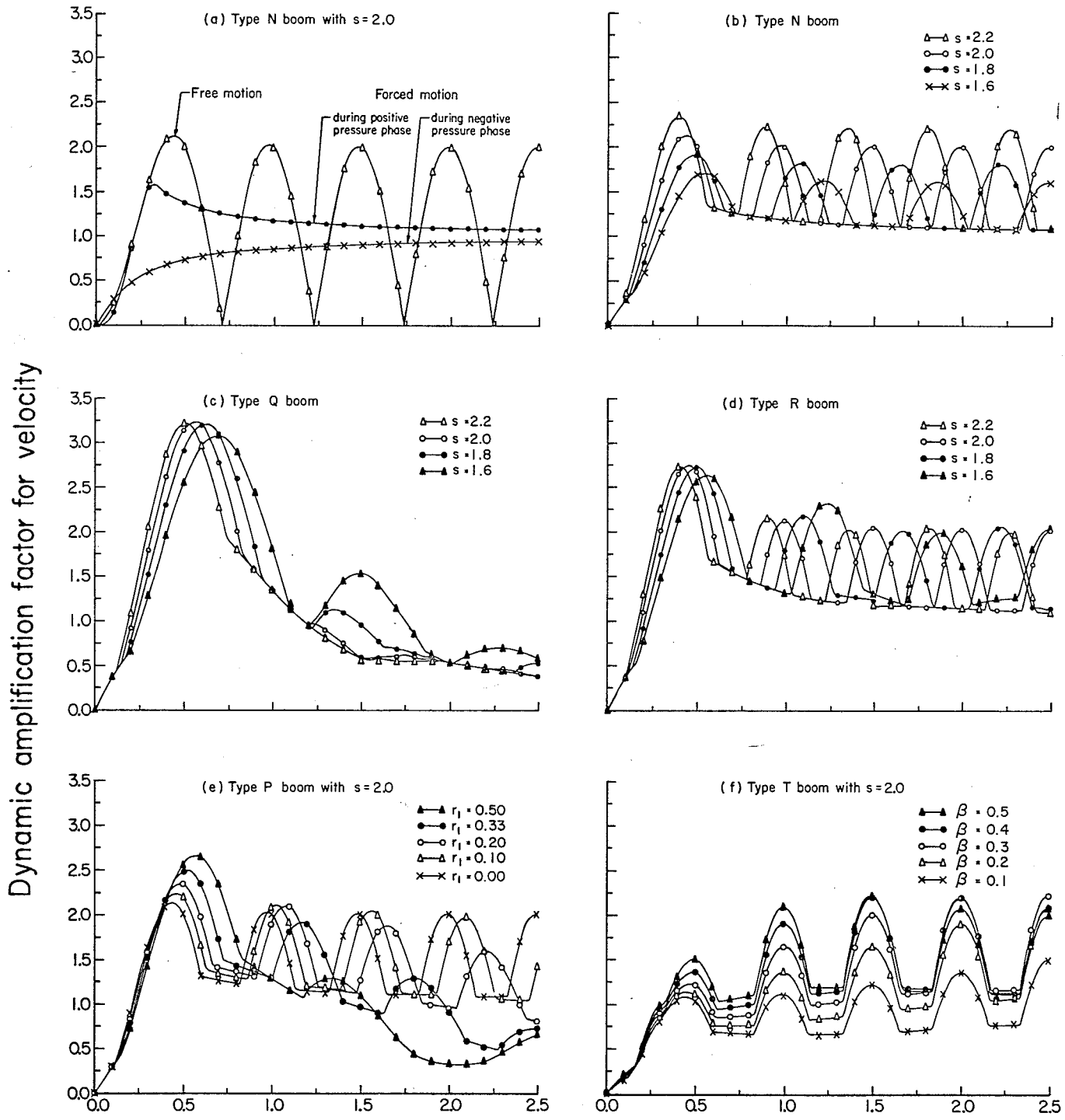

Figure 2. Showing dynamic amplification factors of velocities produced by typical sonic booms.

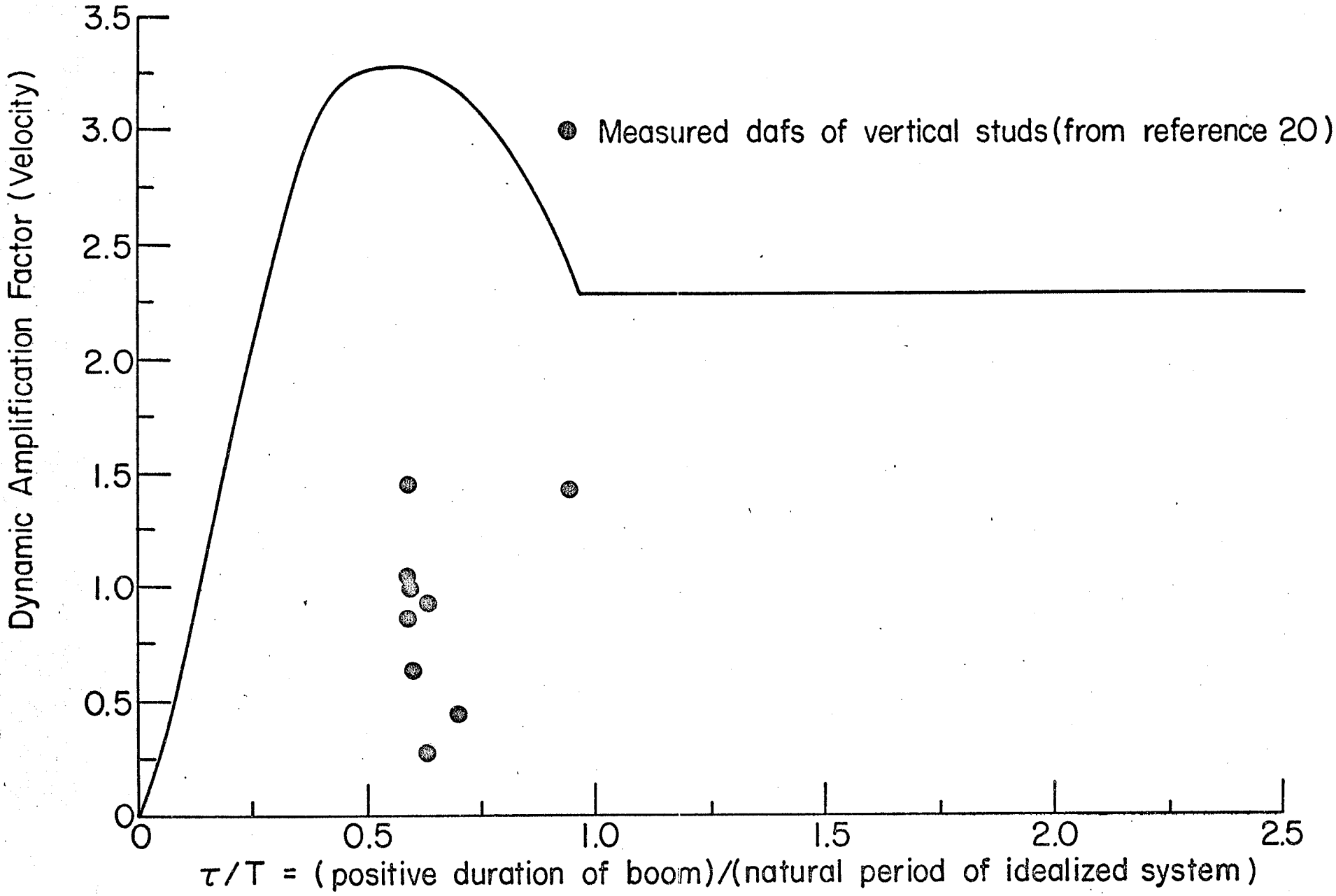

Figure 3. Showing the envelope of dynamic amplification factors.

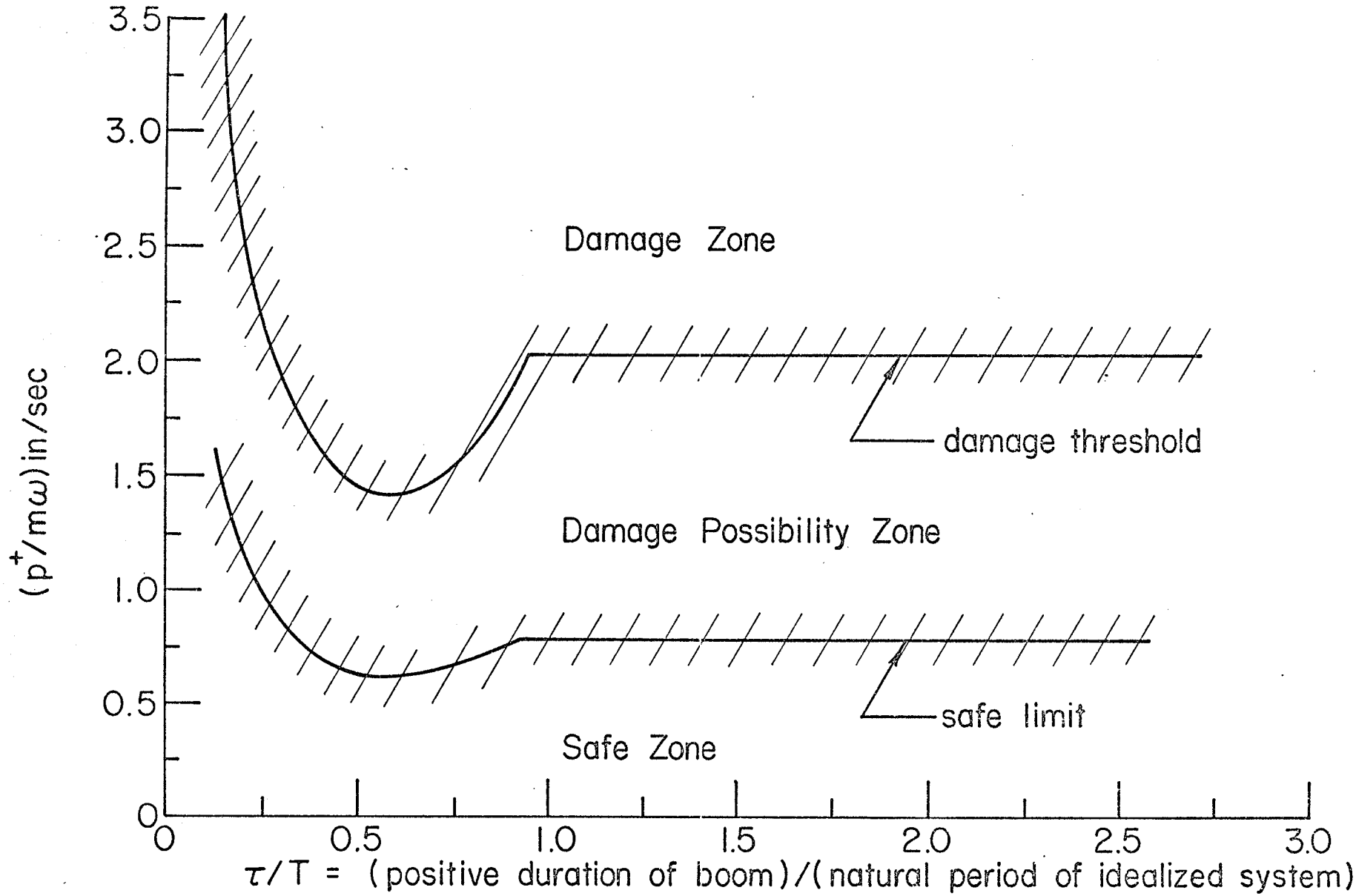

Figure 4. Showing various zones for assessing possible damage of wall-like structural components due to sonic booms.

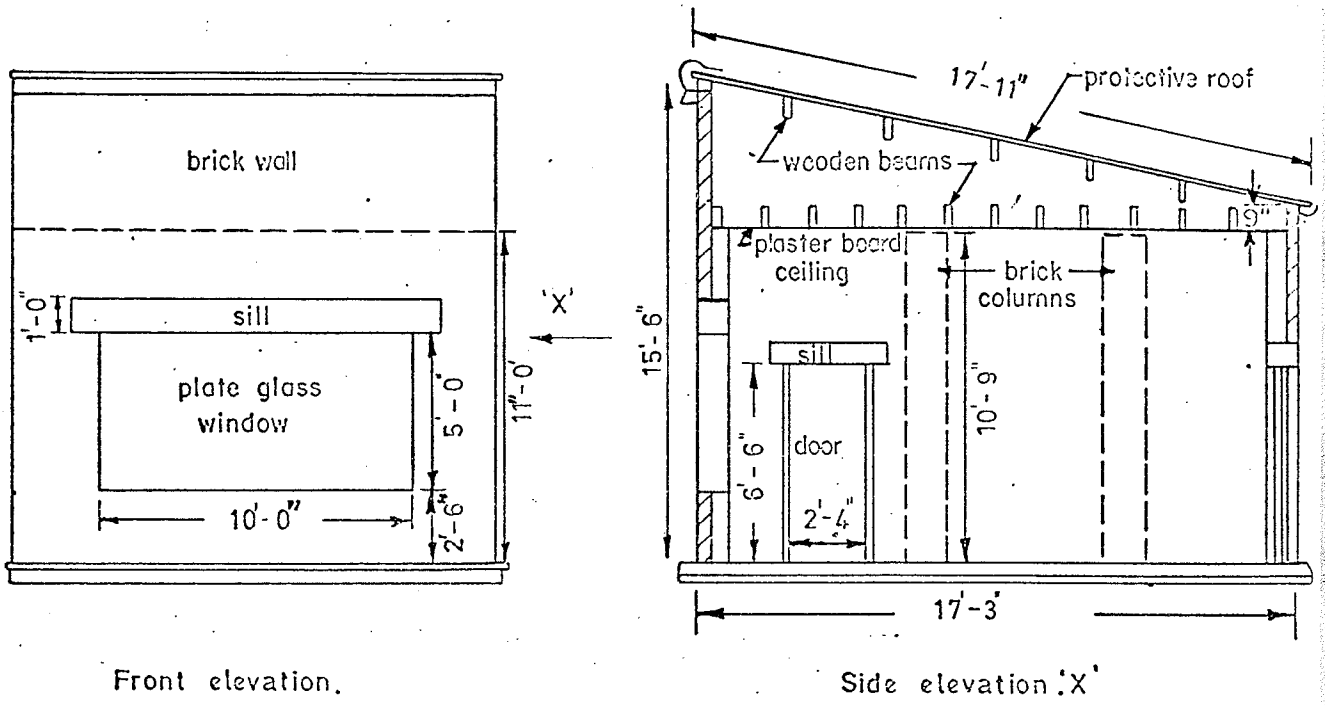

Plan

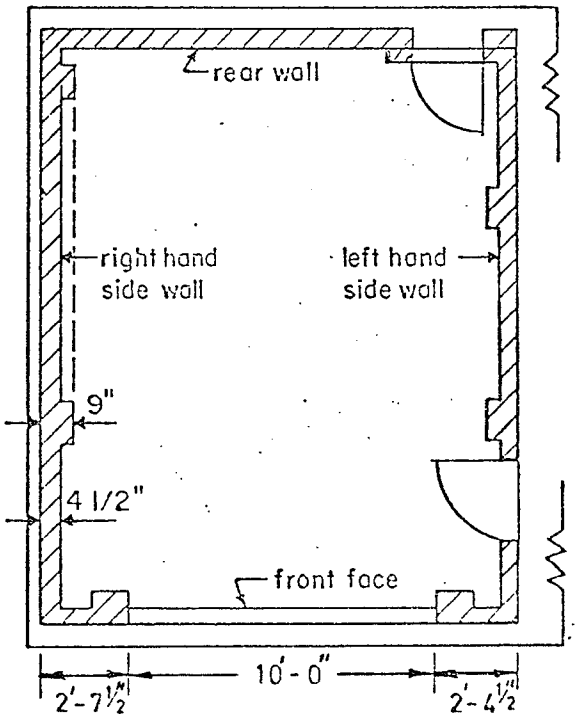

Figure 5. Showing the full-scale structure.

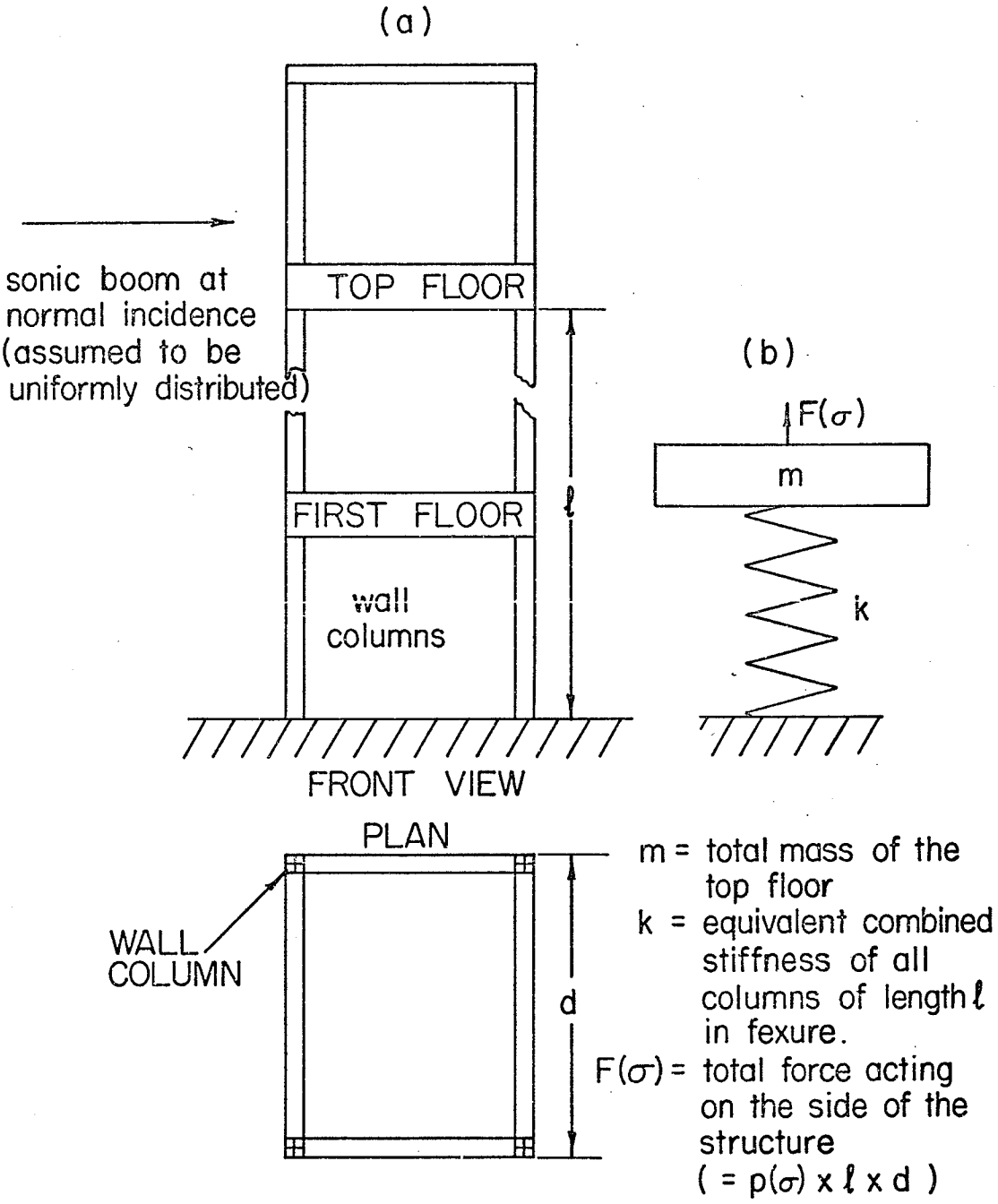

Figure 6. Showing (a) multi-storey building and (b) its idealization .

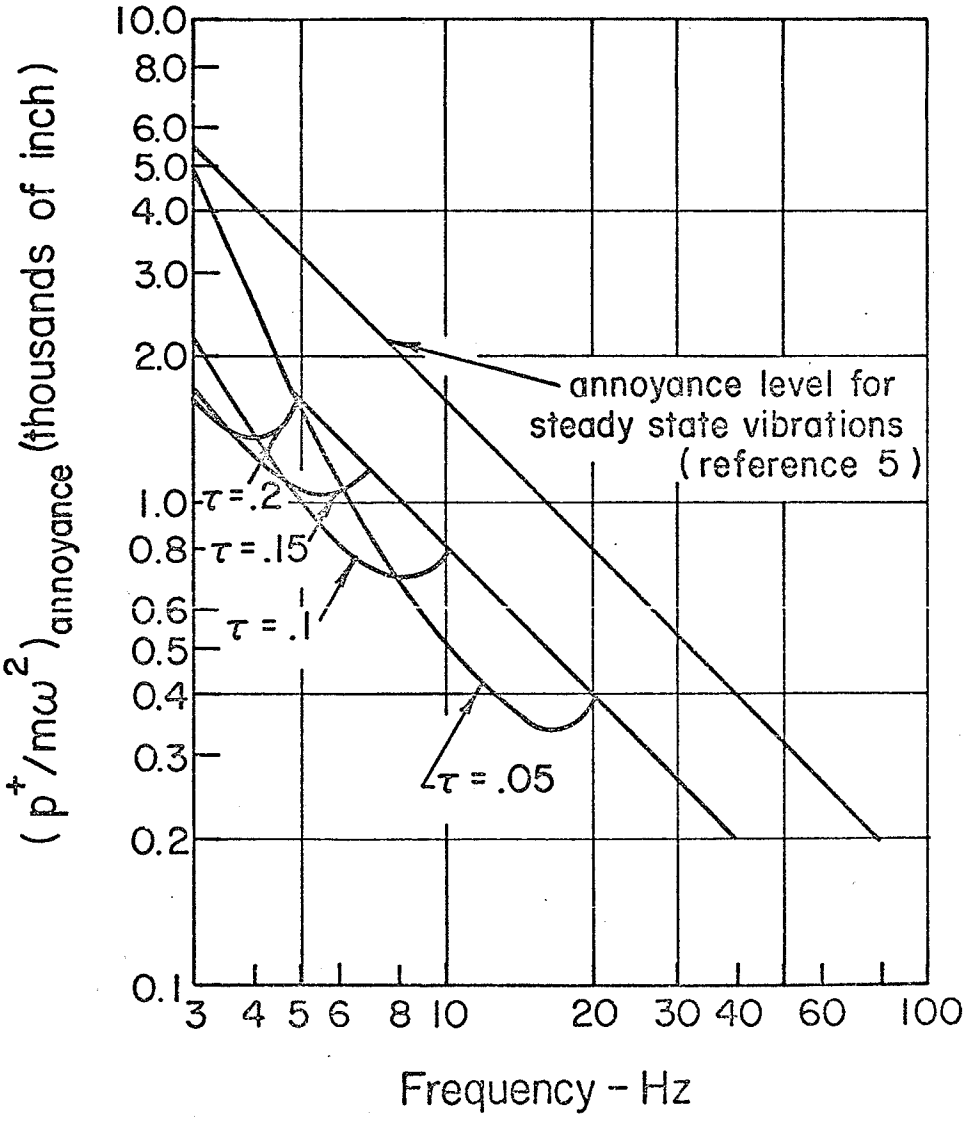

Figure 7. Showing tentative curves assessing the annoyance of people due to vibrations from sonic booms.

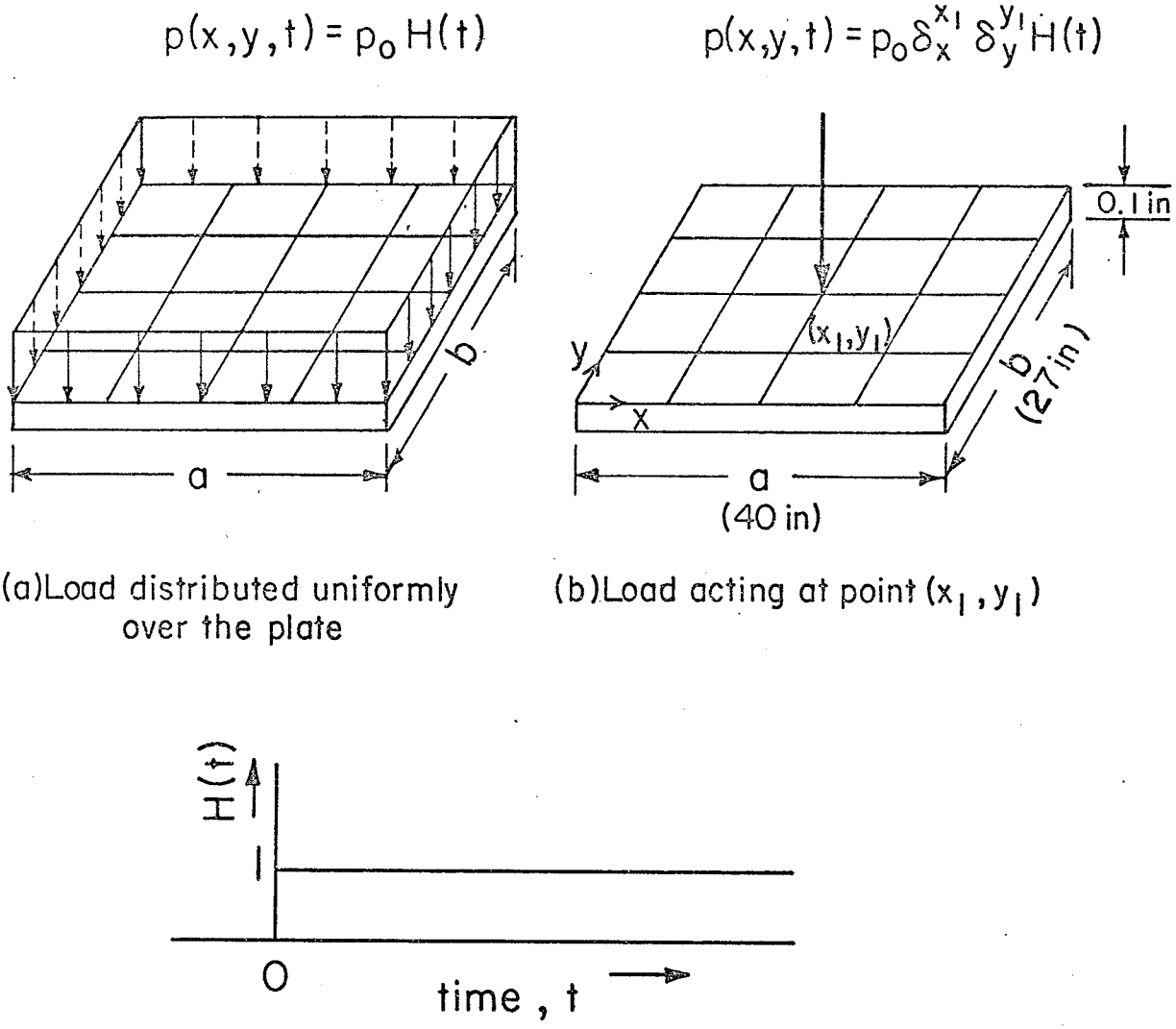

(a)Load distributed uniformly over the plate

(b)Load acting at point (x_1, y_1)

(c) Heaviside's unit step function , H (t)

Figure 8. Showing the two transient loads applied to the simply-supported, rectangular plate.

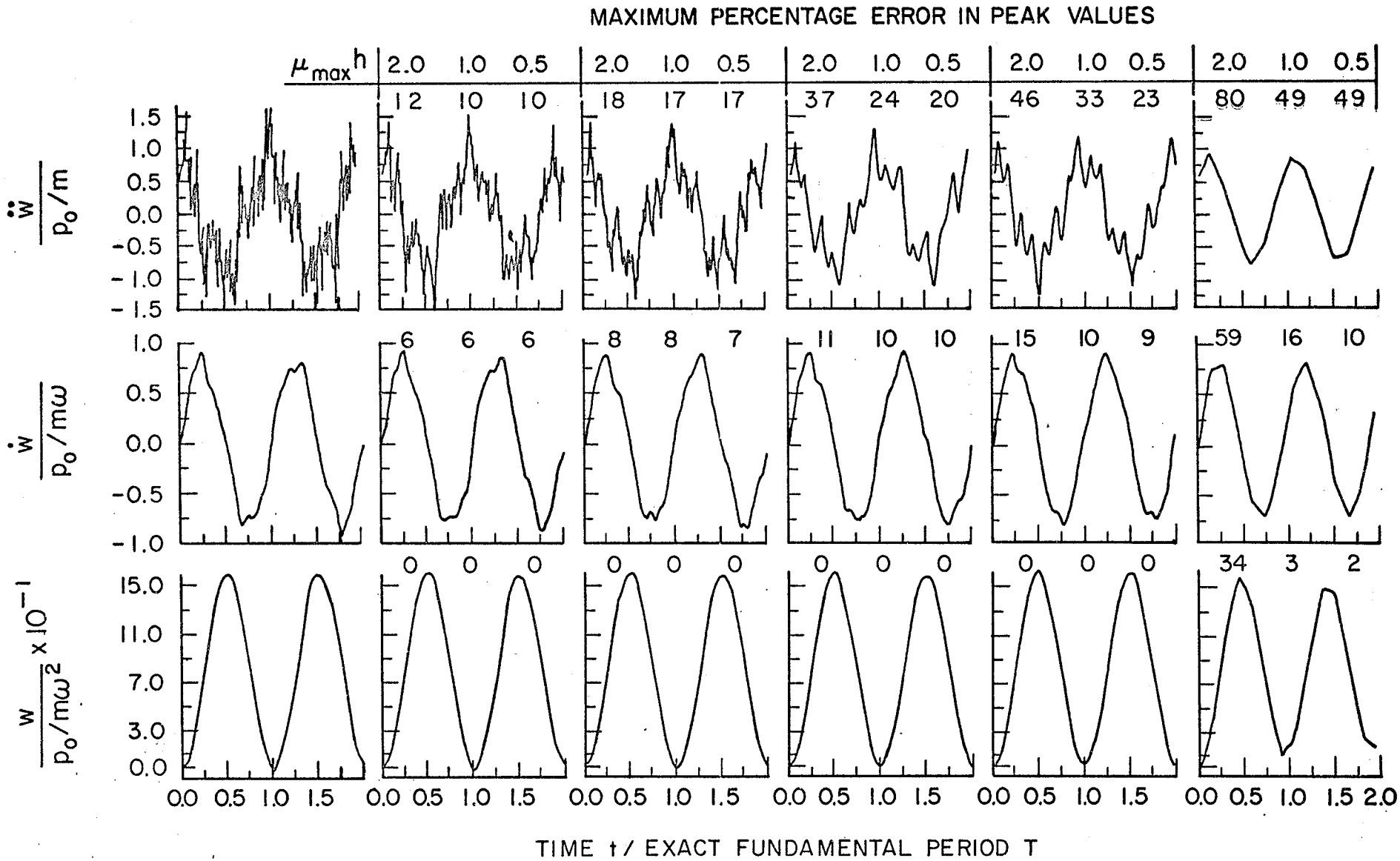

Figure 9. Showing the effects of the elimination technique and step size on the response at the centre of plate due to a uniformly distributed load.

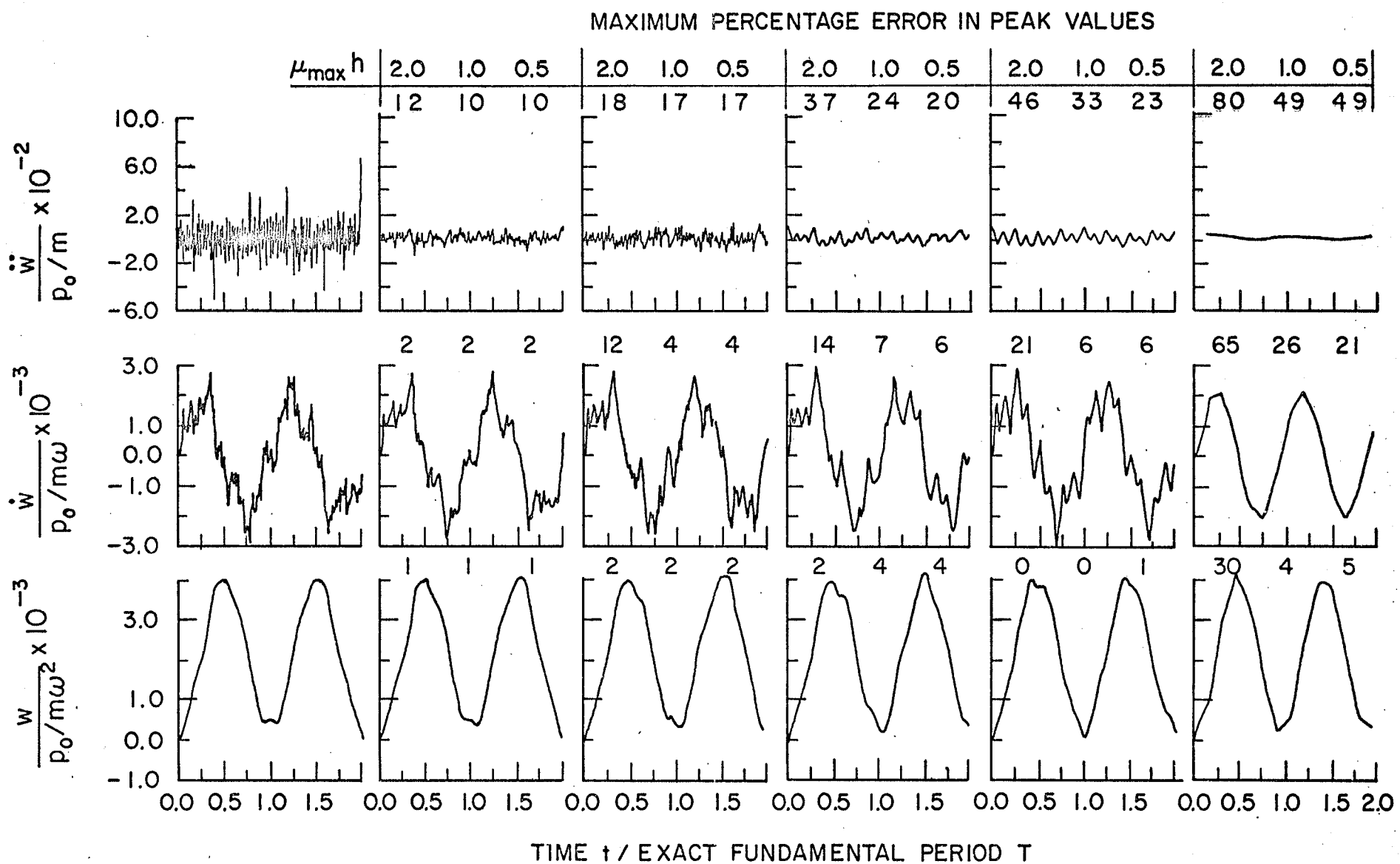

Case (corresponding to free case in Table 2)	Exact	A 1	A5	A6	A9	A11

Figure 10. Showing the effects of the elimination technique and step size on the response at the centre of plate due to a point load.

APPENDIX A

Free motion amplitude, w, in terms of the Fourier Transform of an arbitrary excitation $P(\sigma)$.

From Duhamel's Integral,

$$x(s\tau) = \frac{1}{m\omega} \int_0^{s\tau} P(\sigma) \sin \omega (s\tau - \sigma) \, d\sigma \tag{A.1}$$

and

$$\dot{x}(s\tau) = \frac{1}{m} \int_0^{s\tau} P(\sigma) \cos \omega (s\tau - \sigma) \, d\sigma \tag{A.2}$$

Equations (A.1) and (A.2) give the initial conditions of free vibration when the excitation is terminated. The amplitude of free motion can be written as (27)

$$w(s\tau) = \frac{\dot{x}(s\tau)}{\omega} + i\, x(s\tau). \tag{A.3}$$

Substituting for $x(s\tau)$ and $\dot{x}(s\tau)$ in equations (A.1) and (A.2), respectively, gives

$$w(s\tau) = \frac{e^{i\omega s\tau}}{m\omega} \int_0^{s\tau} P(\sigma) \, e^{-i\omega\sigma} \, d\sigma \tag{A.4}$$

But $P(\sigma) = 0$ for $\sigma < 0$ and $\sigma > s\tau$, so that

$$w(s\tau) = \frac{1}{m\omega} e^{i\omega s\tau} \int_{-\infty}^{\infty} P(\sigma) \, e^{-i\omega\sigma} \, d\sigma \tag{A.5}$$

or

$$|w(s\tau)| = \frac{1}{m\omega} P(\omega) . \tag{A.6}$$

Here $|w(s\tau)|$ is the amplitude of free motion and $P(\omega)$ is the Fourier Transform of the excitation $P(\sigma)$.

APPENDIX B

Theoretical Analysis to Determine the Transient Response

The transverse displacement of a simply-supported rectangular plate can be expressed in terms of the normal modes as (40)

$$w(x,y,t) = \sum\sum_{mn} X_m(x)\, Y_n(y)\, q_{mn}(t) \quad \text{where } m,n = 1,2,3... \tag{B.1}$$

Assuming zero damping, the generalized co-ordinates $q_{mn}(t)$ are given by

$$q_{mn} + \omega^2_{mn} q_{mn} = K_{mn}\, f(t), \tag{B.2}$$

where

$$K_{mn} = \frac{1}{M} \int_0^a \int_0^b p(x,y)\, X_m(x)\, Y_n(y)\, dxdy \tag{B.3}$$

if the excitation is distributed over the face of the plate. M is the mass of the plate; m and n are the mode numbers in x- and y- dimensions of the plate, respectively; and ω_{mn} is the natural frequency of mode m/n. If, on the other hand, the exciting force $P_1 f(t)$ is applied at point (x_1,y_1) then

$$K_{mn} = \frac{P_1}{M} X_m(x_1)\, Y_n(y_1). \tag{B.4}$$

The normal functions $X_m(x)$ and $Y_n(y)$ for a simply-supported plate are

$$X_m(x) = 2^{\frac{1}{2}} \sin \frac{m\pi x}{a}$$

and

$$Y_n(y) = 2^{\frac{1}{2}} \sin \frac{n\pi y}{b}. \tag{B.5}$$

The solution of equation (B.2) is

$$q_{mn} = \frac{K_{mn}}{\omega_{mn}} \int_0^t f(t_1) \sin \omega_{mn}(t-t_1)\, dt_1 \tag{B.6}$$

The displacement is determined from equation (B.6) and (B.1). Then the velocity and acceleration can be evaluated simply by differentiating displacement with respect to time.

APPENDIX C

THE COMPUTER PROGRAMS

Introduction

The computer programs used to calculate the results of Part I and Part II are listed with their specifications. Most subroutines of Part II evolve from the finite element formulation of a rectangular plate written by Mason. Hence the nomenclature is similar to that adopted in the appendix of Mason's Ph.D. thesis (reference 28) except that the dimensioned and actual sizes of arrays (in the dynamic dimensioning) are numerically equal. The subroutines which invert a square matrix, form the product of two matrices and evaluate the eigenvalues and vectors of $(\underline{M} - \lambda\underline{K})\ \{x\} = 0$ are library subroutines. Most of the subroutines involved in determing the transient response have been detailed in the appendices of Ph.D. theses of Craggs and Popplewell (references 27 and 16, respectively). Therefore, all those subroutines not developed by the author are omitted. Figures C.1 and C.2 show the flow diagrams for the free and transient response of a plate considered in Part II.

The specifications in this appendix give the use of the subroutines; quantities passed to the subroutines in the argument list; brief details of the computational procedure and relevant particulars such as data required and the output from the subroutines.

All subroutines for Part II are written in Fortran IV using double precision arithmetic. No computational difficulties were experienced in the eigenvalue subroutine (which employs a QR two-step algorithm) with matrices up to order 82.

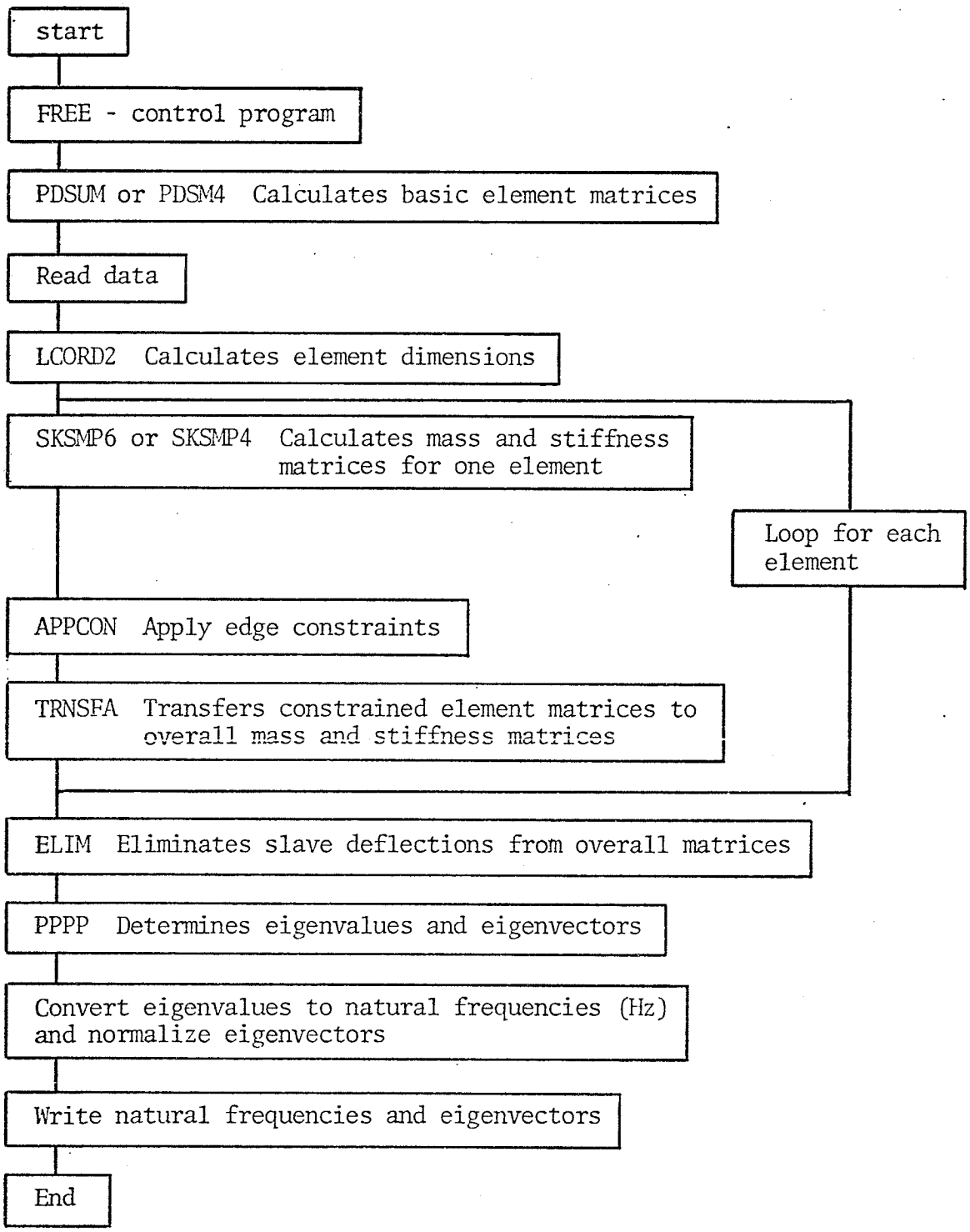

Figure C.1 Flow Diagram of Computer Programs Used for the Determination of Natural Frequencies and Mode Shapes.

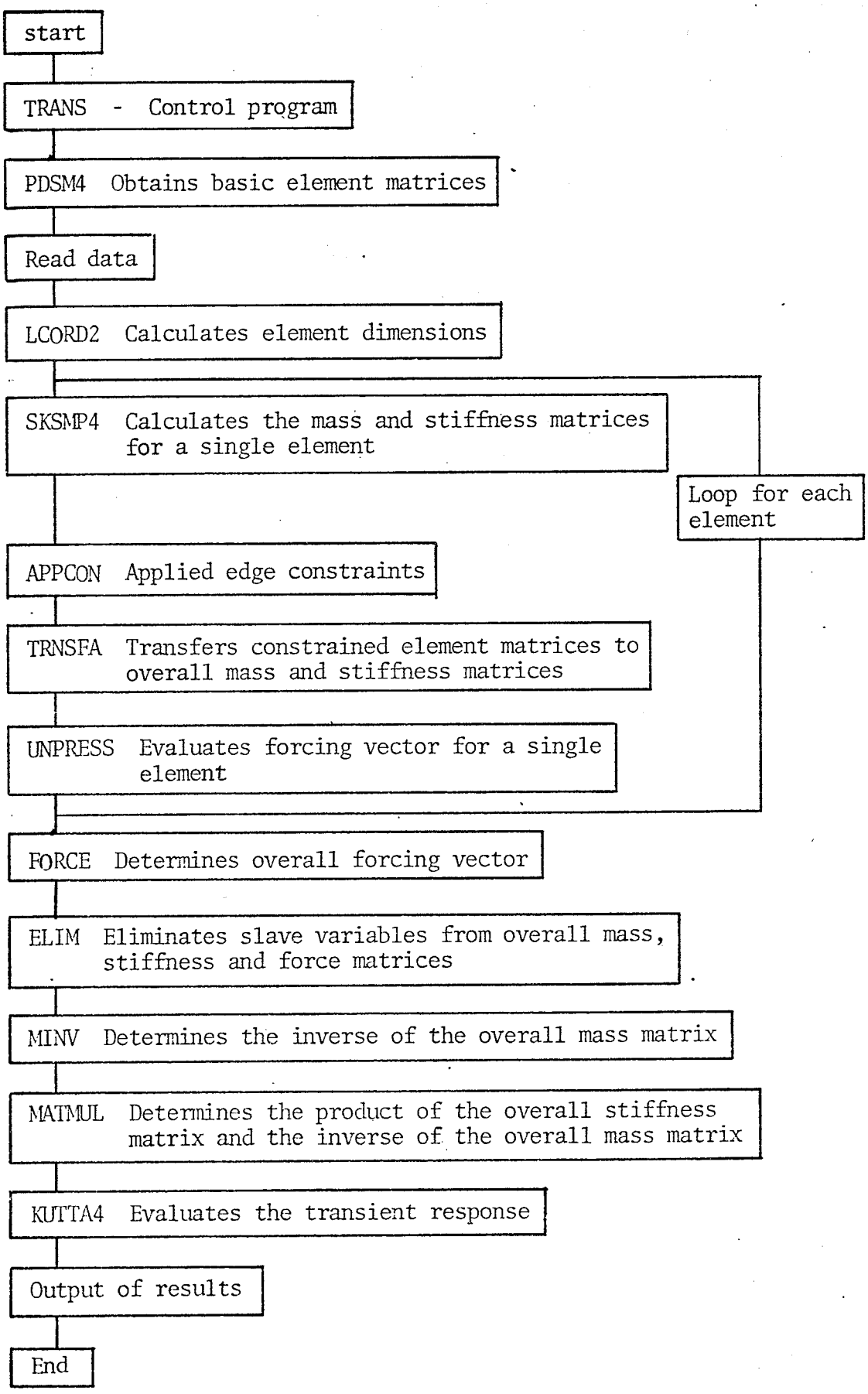

Figure C.2 Flow Diagram of Computer Programs Used for the Determination of Transient Response

SUBROUTINE ELIM

1. Purpose

This subroutine reduces the size of the overall constrained mass, stiffness and force matrices for the complete system by eliminating the selected slave deflections of the system.

2. Argument list

SUBROUTINE ELIM (BKO, BMO, NSUB, NELM, NEL, MSMAL, KSIZE, MSIZE, NP, F).

BMO, BKO and F are the overall constrained mass, stiffness and force matrices, respectively, of the complete system. These are dimensioned as (KSIZE, KSIZE), (KSIZE, KSIZE) and (KSIZE), respectively. NSUB contains the constrained degrees of freedom of each nodal point of the original grid idealization. NELM contains the positions of slave deflections in the complete constrained system. NEL equals the number of slave deflections to be eliminated; MSMAL is the number of degrees of freedom of the reduced system (MSMAL = KSIZE - NEL). NP is the number of nodal points in the grid idealization.

3. Method

NEL slave deflections are eliminated from the mass, stiffness and forces matrices of the complete constrained system in a DO loop. The details of the elimination technique are given in section 2.1.

SUBROUTINE EXAR

1. Purpose

Calculates the 'exact' transient response (displacement velocity and acceleration) of a simply-supported rectangular plate when it is excited by (a) an instantaneous uniform step pressure applied over all the plate and (b) an instantaneous step point load applied at the centre of the plate.

2. Argument list

SUBROUTINE EXAR (DISP, VEL, ACC, T, NIT, NMODE, WMN, A, B, X, Y, XP, YP, IC, EMAX, DT).

DISP, VEL, ACC and T are the arrays which contain displacements, velocities, accelerations and times respectively.

They are all dimensioned as (NIT), where NIT is the total number of time steps considered. NMODE equals the number of lowest frequency modes considered in the computation; WMN contains the natural circular frequencies of the NMODE modes. M and N contain the mode numbers which correspond to each value of WMN. A and B are the dimensions of the plate. X and Y are the global co-ordinates of the point at which the response is determined. XP and YP are the global co-ordinates of the point where the instantaneous step point load acts. EMAX is the value of the natural frequency of the (NMODE) th mode. DT equals the time step for each computation. IC is used to determine whether the loading is of type (a) or (b) above (if IC is not equal to 1, then the loading is uniformly distributed).

3. Method

Details of the method are given in Appendix B of this thesis.

SUBROUTINE FORCE

1. Purpose

To evaluate the constrained forcing vector for a particular grid idealization.

2. Argument list

SUBROUTINE FORCE (F, T, MRED, KS, PNEUO, YMODO, THICKO, PR, KE, KSUBEL).

F is the constrained forcing vector with dimension MRED. KS equals MRED; PR and KSUBEL are described in subroutine UNPRES (see appendix of Popplewell's Ph.D. thesis, reference 16). PNEUO, YMODO and THICKO are standard quantities of the plate's Poisson's ratio, Young's modulus and thickness, respectively. T is the time variable. KE is the actual number of elements in the grid idealization.

3. Method

The constrained forcing vector is assembled manually to allow for different plate's edge constraints. Two examples are presented which corrospond to (a) an instantaneous uniform step pressure all over the plate and (b) instantaneous step point load applied at the geometrical centre of the plate. Details of the formulation of the forcing vector are given in chapter 3 of reference (16).

4. Other subroutines used

UNPRES (indirectly).

SUBROUTINE FREE

1. Purpose

This is the controlling subroutine for the calculation of a plate's free response. Rectangular finite elements with four and six unknowns per corner, respectively, are used together with normal storage of the matrices.

2. Argument list

SUBROUTINE FREE (G, NGE, NC, X, Y, MCN, EV, VAB, EXACT, ERROR, NSUB, KCEM, NE, NP, MSIZE, BMO, BKO, NEL, NELM, NM).

G contains the x and y co-ordinates of the plate's nodal points. NGE contains the nodal point numbers associated with the corner of each plate element. The number of edge constraints for each element are stored in array NC. X and Y are calculated in subroutine LCORD2 and contain the x and y dimensions of each plate element. MCN is the array of NM constraint numbers for each element. EV and VAB provide storage for the computed natural frequencies and mode shapes. They are dimensioned (MSIZE) and (MSIZE, MSIZE), respectively; MSIZE is the number of total constrained degrees of freedom of the plate system. EXACT contains the lowest 100 exact natural frequencies of the simply supported plate. ERROR stores the percentage error computed for each natural frequency. An array NSUB contains the constrained degrees of freedom of each nodal point. KCEM contains the constrained degrees of freedom of corners associated with each element. NE and NP are the actual number of elements and nodal points in a grid idealization. BMO and BKO are the square arrays used to store the mass and stiffness matrices of the plate. They are dimensioned (MSIZE, MSIZE). NEL is the number of slave deflections. NELM contains the positions of NEL slave deflections in the complete constrained system of the plate.

3. Method

Details of the method are given in Mason's Ph.D. thesis, reference (28).

4. Other routines used

PDSM4, PDSUM, LCORD2, SKSMP4, SKSMP6, APPCON, TRNSFA, ELIM, PPPP.

SUBROUTINE TRANS

1. Purpose

This is the controlling subroutine for the calculation of a plate's transient response. Rectangular finite elements with four unknowns per corner are used together with normal storage of the matrices.

2. Argument list

SUBROUTINE TRANS (BMO, BKO, C1, X1, V, VO, V1,
V2, V3, TX, TV, F, ACC, NX, E, PR, NELM, NSUB, NEL, MAX,
TMAX, MIN, TMIN, MRED, NE, NP, NSIZE, PNEUO, THICKO, YMODO).

BMO and BKO are the square arrays used to store the mass and stiffness matrices of the complete constrained system of a rectangular plate. C1 contains the product of the stiffness matrix and the inverse of the mass matrix. X1, V and ACC contain the displacement, velocity and acceleration vectors at any instant (which is multiple of the time step size E). VO, V1, V2, V3, TX, TV are the working spaces of dimension (MSIZE). F is the forcing vector of dimension MSIZE. NX is the total number of time increments. NSUB contains the constrained degrees of freedom of each nodal point. NEL is the total number of slave deflections and NELM contains the positions of their deflections in the original overall constrained system. MAX, MIN, TMAX, TMIN are the values of maximum and minimum responses and their corresponding instants of time, respectively. NE and NP are the number of elements and nodal points in a grid idealization. PNEUO, THICKO and YMODO are the standard quanties of the plate's Poisson's ratio, thickness and Young's modulus, respectively.

3. Method

Outlined in section 2.1.

4. Other routines used

Indirectly - PDSM4, SKSMP4, APPCON, TRNSFA, UNPRESS.
Directly - FORCE, ELIM, MINV, MATMUL, KUTTA4

5. Restrictions

The subroutine is for undamped motion but damped motion may be considered. No alterations are necessary if the damping is made proportional to either the stiffness or mass matrix. (The alterations coming into D2XBDT).

6. Miscellaneous

Since the same grid idealization of the rectangular plate was employed for all the cases considered, the overall constrained mass and stiffness matrices were stored on disk. (Hence, the subroutines involved are used indirectly). The results obtained from

subroutine UNPRES were similarily stored for subsequent use.

SUBROUTINE TRNSFA

1. Purpose

This subroutine transfers the constrained mass and stiffness matrices of a single element to overall constrained mass and stiffness matrices for the complete system.

2. Argument list

SUBROUTINE TRNSFA (BMO, BKO, SM, SK, NGE, IE, KE, KSIZE, N, NSUB, NCORN, NTCOR, KROP1, KROP2, NP, KCEM, NES).

BMO and BKO are the overall constrained (as edge constraints are applied at the elemental level) mass and stiffness matrices, respectively. They are dimensioned as (KSIZE, KSIZE) where KSIZE is the total constrained degrees of freedom of the grid idealization. SM and SK are the element mass and stiffness matrices, respectively, of size (NES, NES),where NES equals the unconstrained degrees of freedom of the element IE. NGE contains the global nodal points associated with the corners of each element. KE is the actual number of elements in the grid idealization; N equals the constrained degrees of freedom of the element IE; NSUB is the number of constrained degrees of freedom per corner; NCORN and NTCOR always equal 4 and 3, respectively. KROP1 and KROP2 are used to determine whether element IE is rectangular or triangular. NP is the actual number of nodal points of the grid idealization; KCEM contains the constrained degrees of freedom of each corner of the element IE.

3. Method

Constrained element matrices are transferred to the overall matrices. Arrays NGE, NSUB and KCEM are used to give the position within the overall matrices to which element matrices are transferred.

4. Miscellaneous

This subroutine is used normally in a loop with subroutines SKSMP4 (or SKSMP6) and APPCON. The element mass and stiffness matrices of an element are calculated using SKSMP4 (or SKSMP6) and APPCON applies the edge constraints to the element matrices before they are transferred to the overall matrices.

SUBROUTINE VELDAF

1. Purpose

To determine the velocity dynamic amplification factors (dafs) of an undamped linear oscillator when it is subjected to the sonic booms shown in Figure 1(b).

2. Argument list

SUBROUTINE VELDAF (FTLMT, DFTOU, NT, AMAXF, AMINF, AFREE, A, FTOU, KOM, NR, NSET).

FTLMT is the highest value of FTOU (i.e. τ/T) considered (2.5). DFTOU is the increment in τ/T. NT is the total number of increments considered. AMAXF, AMINF and AFREE are the arrays which are used to store the absolute values of the maximum non-dimensionalized velocities produced during positive pressure, negative pressure and free motion phases, respectively, for each value of FTOU. They each have dimension NT. Array A provides storage for the greatest of the AMAXF, AMINF and AFREE dafs. FTOU contains the different values of τ/T considered and has dimension NT. KOM is used to determine the type of sonic boom considered (the numbers 1, 2, 3, 4 and 5 correspond to the type N, P, Q, R and T booms, respectively). NR always equals 1. NSET is the number of cases (due to variations in a sonic boom) considered in one set of computation.

3. Method

The details of the method are given in section 1.3.

```
      SUBROUTINE FLIM (BKC,BMC,NSUB,NELM,NEL,MSMAL,KSIZE,MSIZE,NP,F)
      IMPLICIT REAL*8(A-H,O-Z),INTEGER(I-N)
      DIMENSION BKC(KSIZE,KSIZE),BMC(KSIZE,KSIZE),NSUB(NP),NELM(NEL)
      DIMENSION F(KSIZE)
      MSMAL=KSIZE
      IF(NEL.LT.2) GO TO 1
      DO 1 I=1,NEL
      NS=NELM(I)-I+1
      BKS=BKC(NS,NS)
      FFFFF=F(NS)
      DO 2 L=1,MSMAL
      F(L)=F(L)-FFFFF*BKC(L,NS)/BKC(NS,NS)
      DO 2 M=1,MSMAL
      IF(L.EQ.NS) GO TO 4
      IF(M.EQ.NS) GO TO 4
      BKC(L,M)=BKC(L,M)-BKC(L,NS)*BKC(M,NS)/BKC(NS,NS)
      BMC(L,M)=BMC(L,M)-BMC(L,NS)*BKC(M,NS)/BKC(NS,NS)-BMC(M,NS)*BKC(L,
     *NS)/BKC(NS,NS)+BMC(NS,NS)*BKC(L,NS)*BKC(M,NS)/(BKC(NS,NS)*BKC(NS,
     *NS))
    4 CONTINUE
    2 CONTINUE
      MSMAL=MSMAL-1
      DO 1 L=1,MSMAL
      J=L
      IF(L.GE.NS) J=L+1
      F(L)=F(J)
      DO 1 M=1,MSMAL
      K=M
      IF(M.GE.NS) K=M+1
      BKC(L,M)=BKC(J,K)
      BMC(L,M)=BMC(J,K)
    1 CONTINUE
      RETURN
      END
```

```
      SUBROUTINE EXAR(DISP,VEL,ACC,T,NIT,NMODE,M,N,WMN,A,B,XP,YP,X,Y,IC)
      DIMENSION DISP(NIT),VEL(NIT),ACC(NIT),T(NIT),
     *M(NMODE),N(NMODE),WMN(NMODE),WK(NMODE),W1(NMODE)
      A=40.0
      B=27.0
      XP=20.0
      YP=13.5
      RHE=0.15/386.4
      READ(5,103) IC
  103 FORMAT(I5)
      READ(5,101) NMODE,NT,IPOINT,DT
  101 FORMAT(3I10,F10.0)
      DO 1 I=1,NMODE
    1 READ(5,100) M(I),N(I),WMN(I)
  100 FORMAT(2I10,F16.7)
      EMAX=WMN(NMODE)
      DT=1.0/EMAX
      NT=2.0/(DT*1.46051)
      IP=1
   15 READ(5,102) X,Y
  102 FORMAT(2F10.0)
      API=2576.0/9.8696044
      T(1)=0.0
      DO 2 J=1,NT
      DISP(J)=0.0
      VEL(J)=0.0
      ACC(J)=0.0
      IF(J.EQ.1) GO TO 16
      T(J)=T(J-1)+DT
   16 CONTINUE
      DO 3 I=1,NMODE
      AM=M(I)
      AN=N(I)
      IF(IC.EQ.1) GO TO 21
      WK(I)=API/(AM*AN)*(1.0-COS(AM*3.14159  ))*(1.0-COS(AN*3.14159  ))
      GO TO 22
   21 CONTINUE
      WK(I)=2576.0/1080.0*SIN(AM*3.14159  *XP/A)*SIN(AN*3.14159  *YP/B)
   22 CONTINUE
      W1(I)=2.0*SIN(AM*3.14159  *X/A)*SIN(AN*3.14159  *Y/B)
      DISP(J)=DISP(J)+WK(I)*W1(I)*(1.0-COS(WMN(I)*T(J)))/(WMN(I))**2.0
      VEL(J)=VEL(J)+WK(I)*W1(I)*SIN(WMN(I)*T(J))/WMN(I)
      ACC(J)=ACC(J)+WK(I)*W1(I)*COS(WMN(I)*T(J))
    3 CONTINUE
      ACC(J)=ACC(J)/386.4
      DISP(J)=DISP(J)*RHE*WMN(1)*WMN(1)
      VEL(J)=VEL(J)*RHE*WMN(1)
      ACC(J)=ACC(J)*RHE*386.4
    2 CONTINUE
      IP=IP+1
      IF(IP.GT.IPOINT) GO TO 18
      GO TO 15
   18 CONTINUE
      RETURN
      END
```

```
      SUBROUTINE FORCE (F,T,MRED,KS,PNEUO,YMODC,THICKO,PR,KE,KSUBEL)
      DIMENSION PR(KE,16,1),NSUB(NP),F(MSIZE)
    4 FORMAT(8F12.3)
      DO 10 I=1,KS
   10 F(I)=0.0
      READ(5,51) NF
   51 FORMAT(I5)
      NP=31
      IF(NF.EQ.1) GO TO 12
      F(1)=PR(4,1,1)
      F(2)=PR(11,1,1)+PR(3,2,1)
      F(3)=PR(12,1,1)+PR(4,2,1)
      F(4)=PR(11,2,1)+PR(3,3,1)
      F(5)=PR(12,2,1)+PR(4,3,1)
      F(6)=PR(11,3,1)+PR(3,4,1)
      F(7)=PR(12,3,1)+PR(4,4,1)
      F(8)=PR(12,4,1)
      F(9)=PR(6,1,1)+PR(2,5,1)
      F(10)=PR(8,1,1)+PR(4,5,1)
      F(11)=PR(13,1,1)+PR(5,2,1)+PR(9,5,1)+PR(1,6,1)
      F(12)=PR(14,1,1)+PR(6,2,1)+PR(10,5,1)+PR(2,6,1)
      F(13)=PR(15,1,1)+PR(7,2,1)+PR(11,5,1)+PR(3,6,1)
      F(14)=PR(16,1,1)+PR(8,2,1)+PR(12,5,1)+PR(4,6,1)
      F(15)=PR(13,2,1)+PR(5,3,1)+PR(9,6,1)+PR(1,7,1)
      F(16)=PR(14,2,1)+PR(6,3,1)+PR(10,6,1)+PR(2,7,1)
      F(17)=PR(15,2,1)+PR(7,3,1)+PR(11,6,1)+PR(3,7,1)
      F(18)=PR(16,2,1)+PR(8,3,1)+PR(12,6,1)+PR(4,7,1)
      F(19)=PR(13,3,1)+PR(5,4,1)+PR(9,7,1)+PR(1,8,1)
      F(20)=PR(14,3,1)+PR(6,4,1)+PR(10,7,1)+PR(2,8,1)
      F(21)=PR(15,3,1)+PR(7,4,1)+PR(11,7,1)+PR(3,8,1)
      F(22)=PR(16,3,1)+PR(8,4,1)+PR(12,7,1)+PR(4,8,1)
      F(23)=PR(14,4,1)+PR(10,8,1)
      F(24)=PR(16,4,1)+PR(12,8,1)
      F(25)=PR(6,5,1)+PR(2,9,1)
      F(26)=PR(8,5,1)+PR(4,9,1)
      F(27)=PR(13,5,1)+PR(5,6,1)+PR(9,9,1)+PR(1,10,1)
      F(28)=PR(14,5,1)+PR(6,6,1)+PR(10,9,1)+PR(2,10,1)
      F(29)=PR(15,5,1)+PR(7,6,1)+PR(11,9,1)+PR(3,10,1)
      F(30)=PR(16,5,1)+PR(8,6,1)+PR(12,9,1)+PR(4,10,1)
      F(31)=PR(13,6,1)+PR(5,7,1)+PR(9,10,1)+PR(1,11,1)
      F(32)=PR(14,6,1)+PR(6,7,1)+PR(10,10,1)+PR(2,11,1)
      F(33)=PR(15,6,1)+PR(7,7,1)+PR(11,10,1)+PR(3,11,1)
      F(34)=PR(16,6,1)+PR(8,7,1)+PR(12,10,1)+PR(4,11,1)
      F(35)=PR(13,7,1)+PR(5,8,1)+PR(9,11,1)+PR(1,12,1)
      F(36)=PR(14,7,1)+PR(6,8,1)+PR(10,11,1)+PR(2,12,1)
      F(37)=PR(15,7,1)+PR(7,8,1)+PR(11,11,1)+PR(3,12,1)
      F(38)=PR(16,7,1)+PR(8,8,1)+PR(12,11,1)+PR(4,12,1)
      F(39)=PR(14,8,1)+PR(10,12,1)
      F(40)=PR(16,8,1)+PR(12,12,1)
      F(41)=PR(6,9,1)+PR(2,13,1)
      F(42)=PR(8,9,1)+PR(4,13,1)
      F(43)=PR(13,9,1)+PR(5,10,1)+PR(9,13,1)+PR(1,14,1)
      F(44)=PR(14,9,1)+PR(6,10,1)+PR(10,13,1)+PR(2,14,1)
      F(45)=PR(15,9,1)+PR(7,10,1)+PR(11,13,1)+PR(3,14,1)
      F(46)=PR(16,9,1)+PR(8,10,1)+PR(12,13,1)+PR(4,14,1)
      F(47)=PR(13,10,1)+PR(5,11,1)+PR(9,14,1)+PR(1,15,1)
```

```
      F(48)=PP(14,10,1)+PR(6,11,1)+PR(10,14,1)+PR(2,15,1)
      F(49)=PR(15,10,1)+PR(7,11,1)+PR(11,14,1)+PR(3,15,1)
      F(50)=PR(16,10,1)+PR(8,11,1)+PR(12,14,1)+PR(4,15,1)
      F(51)=PR(13,11,1)+PR(5,12,1)+PR(9,14,1)+PR(1,16,1)
      F(52)=PR(14,11,1)+PR(6,12,1)+PR(10,15,1)+PR(2,16,1)
      F(53)=PR(15,11,1)+PR(7,12,1)+PR(11,15,1)+PR(3,16,1)
      F(54)=PR(16,11,1)+PR(8,12,1)+PR(12,15,1)+PR(4,16,1)
      F(55)=PR(14,12,1)+PR(10,16,1)
      F(56)=PR(16,12,1)+PR(12,16,1)
      F(57)=PR(8,13,1)
      F(58)=PR(15,13,1)+PR(7,14,1)
      F(59)=PR(16,13,1)+PR(8,14,1)
      F(60)=PR(15,14,1)+PR(7,15,1)
      F(61)=PR(16,14,1)+PR(8,15,1)
      F(62)=PR(15,15,1)+PR(7,16,1)
      F(63)=PR(16,15,1)+PR(8,16,1)
      F(64)=PR(16,16,1)
   12 IF(NF.EQ.1) F(NP)=1.0
      DO 11 J=1,KS
      F(J)=F(J)*((12.0*(1.0-PNEU0**2))/(YMOD0*(THICK0**3)))
   11 CONTINUE
      WRITE(6,4) (F(I),I=1,KS)
      RETURN
      END
```

```
      SUBROUTINE FREE (G,NGE,NC,X,Y,MCN,EV,VAB,EXACT,ERROR,NSUB,
     *KCEM,NE,NP,MSIZE,BMO,BKO,NEL,NELM,NM)
      DIMENSION G(NP,2),NGE(NE,4),X(NE),Y(NE),MCN(NE,NM),NC(NE),
     *EV(MSIZE),EXACT(100),ERROR(100),NSUB(NP),KCEM(NE,4),
     *BMO(MSIZE,MSIZE),BKO(MSIZE,MSIZE),VAB(MSIZE,MSIZE),NELM(NEL)
      WRITE(6,606)
      READ(5,1) ICHECK
      IF(ICHECK.EQ.1) GO TO 700
      CALL PDSUM(PI,PS1,PS2,PS3,PS4)
      GO TO 701
  700 CALL PDSM4 (PI,PS1,PS2,PS3,PS4)
  701 CONTINUE
      READ(5,29) PNEUO,RHOO,YMODO,THICKO
      READ(5,29) PNEU,RHO,YMOD,THICK
      WRITE(6,606)
      WRITE(6,606)
   29 FORMAT(4F20.0)
      READ(5,30) (EXACT(I),I=1,100)
   30 FORMAT(5F16.0)
      READ(5,3) NE,NP,KS,NES
      DO 111 I=1,NE
  111 READ(5,1) NC(I),NNC,(MCN(I,J),J=1,NNC)
      READ(5,78) (NSUB(I),I=1,NP)
      DO 995 I=1,NE
  995 READ(5,78) (KCEM(I,J),J=1,4)
      READ(5,1) NEL
      IF(NEL.LT.1) GO TO 119
      READ(5,1) (NELM(I),I=1,NEL)
  119 CONTINUE
   78 FORMAT(16I5)
      DO 112 I=1,NE
  112 KC(I)=NC(I)
    1 FORMAT(16I5)
      KE=NE
      KP=NP
      READ(5,3) KROP1,KROP2,KROP3
   88 FORMAT(2I5)
    3 FORMAT(4I5)
      MSIZE=KS
      READ(5,11) KSIZE,((NGE(I,J),J=1,4),I=1,NE)
  606 FORMAT('  TESRING')
      WRITE(6,606)
   11 FORMAT(I5/(4I5))
      DO 4 I=1,KSIZE
      DO 4 J=1,KSIZE
      BMO(I,J)=0.0D0
    4 BKO(I,J)=0.0D0
      DO 593 I=1,NE
      X(I)=0.0D0
  593 Y(I)=0.0D0
      READ(5,221) ((G(I,J),J=1,2),I=1,NP)
      WRITE(6,606)
  221 FORMAT(2F10.0)
      TN=32.0D0
      FM=1.0D0
      FK=1.0D0
```

```
      CALL LCORD2(1,NE,KE,NP,KP,NGE,G,X,Y,KROP2,KROP3)
      WRITE(6,629) NE,NP,KS,KC,KSIZE,MSIZE
  629 FORMAT(6I5)
      DO 5 L=1,NE
      NNC=NC(L)
      IF(ICHECK.NE.1) GO TO 743
      CALL SKSMP4(PI,PS1,PS2,PS3,PS4,SK,SM,NE,KE,X,Y,L,PNEU,RFC,YMOD,
     *THICK,PNEUO,RFCO,YMODO,THICKO)
      GO TO 702
  743 CALL SKSMP6(PI,PS1,PS2,PS3,PS4,SK,SM,NE,KE,X,Y,L,PNEU,RFC,YMOD,
     *THICK,PNEUO,RFCO,YMODO,THICKO)
  702 CONTINUE
      MRED=NES
      IF(ICHECK.EQ.1) GO TO 703
      CALL APPCON(SM,SK,MCN,24,NNC,MREC,24,L,NE)
      GO TO 704
  703 CONTINUE
      CALL APPCON(SM,SK,MCN,16,NNC,MREC,16,L,NE)
  704 CONTINUE
      CALL TRNSFA(BMC,BKC,SM,SK,NGE,L,KE,KSIZE,MRED,NSUB,4,3,KROP1,KROP
     *2,NP,KCEM,NES)
    5 CONTINUE
      MSMAL=KSIZE
      IF(NEL.LT.1) GO TO 121
      CALL ELIM(BKC,BMO,NSUB,NELM,NEL,MSMAL,KSIZE,MSIZE,NP)
  121 CONTINUE
      MRED=MSMAL
      NV=MRED
      DO 91 NA=1,MRED
      DO 91 NB=1,MRED
      BMO(NA,NB)=FM*BMO(NA,NB)
   91 BKC(NA,NB)=BKC(NA,NB)*FK
      WRITE(6,753) MRED
  753 FORMAT(I15)
  479 FORMAT(8D15.6)
      CALL PPPP(BKO,BMO,MRED,KS,TN,EV,EVI,VAB,CINV,INDIC,SUBDIA,WORK1,
     *WORK2,WORK,IWORK,LOCAL,PREACT,DET,NV,INS,MSIZE)
      DO 189 L=1,NV
      IF(EV(L).NE.0.0D0) EV(L)=1.0D0/EV(L)
  189 CONTINUE
      IF(DET.NE.0.0D0) GO TO 83
      WRITE(6,303)
  303 FORMAT(5X,'DETERMINANT OF BKO-1 =0.0')
      CALL EXIT
   83 CONTINUE
      DO 10 NA=1,NV
      EV(NA)=EV(NA)*FM/FK
      EV(NA)=DSQRT(EV(NA))
      EV(NA)=EV(NA)/(2.0D0*3.141592654)
      ERROR(NA)=100.0*(EV(NA)-EXACT(NA))/EXACT(NA)
      PRINT 313,EV(NA),ERROR(NA),NA
  313 FORMAT(5X,'FREQUENCY=',D15.7,' C.P.S.',10X,'PERCENTAGE ERROR=',
     *D15.7,I10)
   10 CONTINUE
      RETURN
      END
```

```
      SUBROUTINE TRANS(BMC,BKC,C1,X1,V,V0,V1,V2,V3,TX,TV,F,ACC,
     *NX,E,PR,NELM,
     *NSUB,NEL,MAX,TMAX,MIN,TMIN,MRED,NE,NP,MSIZE,PNEUO,THICKO,YMODO)
      DIMENSION BMC(MSIZE,MSIZE),BKC(MSIZE,MSIZE),C1(MSIZE,MSIZE),
     *X1(MSIZE),V(MSIZE),V0(MSIZE),V1(MSIZE),V2(MSIZE),V3(MSIZE),
     *TX(MSIZE),TV(MSIZE),F(MSIZE),ACC(MSIZE),
     *PR(NE,16,1),NELM(NEL),NSUB(NP)
  400 FORMAT(3I10,2F15.0)
  401 FORMAT(I5)
  402 FORMAT(16I5)
  403 FORMAT(8D15.6)
      REWIND 8
      REWIND 9
      DO 532 I=1,64
  532 READ(8) (BKC(I,J),J=1,64)
      READ(8) MRED,KS,KSIZE,KSUBEL,KE,NE,NP,MSIZE,NSUBEL,PNEU,THICKO,
     *PNEUO,YMODO
      READ(8) (NSUB(I),I=1,25)
      WRITE(6,429) MRED,KS,KSIZE,KSUBEL,KE,NE,NP,MSIZE,NSUBEL,PNEU,
     *THICKO,PNEUO,YMODO
      WRITE(6,430) (NSUB(I),I=1,NP)
  430 FORMAT(16I5)
  429 FORMAT(9I5,4F10.2,I5)
      DO 536 I=1,64
  536 READ(9) (BMC(I,J),J=1,64)
      DO 441 I=1,NE
  441 READ(9) (PR(K,I,1),K=1,16)
      DO 442 I=1,NE
  442 WRITE(6,8) (PR(K,I,1),K=1,16)
    8 FORMAT(8F12.3)
      READ(5,400) NX,NVP,KS,EMAX,XKAY
      E=1.0/(EMAX*6.28318)
      NX=2.0/(E*1.46051)
      T=0.0
      CALL FORCE (F,T,MRED,KS,PNEUO,YMODO,THICKO,PR,KE,KSUBEL)
      READ(5,401) NEL
      IF(NEL.LT.2) GO TO 509
      READ(5,402) (NELM(I),I=1,NEL)
      CALL FLIM (BKC,BMC,NSUB,NELM,NEL,MSMAL,KSIZE,MSIZE,NP,F)
      MRED=MSMAL
  509 CONTINUE
      WRITE(6,403) (F(I),I=1,MRED)
      CALL MINV(BMC,MRED,KSIZE,DET)
  732 FORMAT(I80)
      CALL MATMUL(BMC,BKC,C1,KSIZE,KSIZE,KSIZE,MRED,MRED,MRED)
      DO 500 NIP=1,MRED
      DO 500 NP=1,MRED
      BKC(NIP,NP)=0.0
  500 CONTINUE
      DO 501 NP=1,MRED
  501 BKC(NP,NP)=XKAY
      DO 503 I=1,MRED
      X1(I)=0.0
  503 V(I)=0.0
      WRITE(6,732) MRED
      CALL KUTTA4 (BMC,C1,BKC,X1,V,F,V0,V1,V2,V3,TX,TV,E,MRED,KSIZE,
     1KS,ACC,PR,KE,NX,PNEUO,YMODO,THICKO,KSUBEL,
     *YY,A,TT,NIT,NUT,NVP,MAX,MIN,TMAX,TMIN,CCC,NNN,KKN,NC,AA)
      STOP
      END
```

```
      SUBROUTINE TRNSFA(BMO,BKO,SM,SK,NGE,IE,KE,KSIZE,
     *N,NSUB,NCORN,NTCOR,KROP1,KROP2,NP,KCEM,NES)
      IMPLICIT REAL*8(A-H,C-Z),INTEGER(I-N)
      DIMENSION BMO(KSIZE,KSIZE),BKO(KSIZE,KSIZE),SM(NES,NES),
     *SK(NES,NES),
     *          NGE(KE,NCORN),NSUB(NP),KCEM(KE,NCORN)
      IF(IE.LT.KROP1) GO TO 2
      DO 3 I1=1,NTCOR
      DO 3 I2=1,NTCOR
      NL=NGE(IE,I1)-1
      KSUB=NSUB(NL)
      N3=KSUB*(NGE(IE,I1)-1)
      N4=KSUB*(NGE(IE,I2)-1)
      DO 3 L1=1,KSUB
      DO 3 L2=1,KSUB
      LA=L1+N3
      LB=L2+N4
      IA=L1+(I1-1)*KSUB
      IB=L2+(I2-1)*KSUB
      BMO(LA,LB)=BMO(LA,LB)+SM(IA,IB)
    3 BKO(LA,LB)=BKO(LA,LB)+SK(IA,IB)
      GO TO 1
    2 CONTINUE
      DO 4 I1=1,NCORN
      NL=NGE(IE,I1)-1
      N3=0
      IF(NL.NE.0) GO TO 70
      GO TO 71
   70 CONTINUE
      DO 10 I=1,NL
   10 N3=N3+NSUB(I)
   71 CONTINUE
      KL=I1-1
      N33=0
      IF(KL.NE.0) GO TO 72
      GO TO 73
   72 CONTINUE
      DO 12 I=1,KL
   12 N33=N33+KCEM(IE,I)
   73 CONTINUE
      NLL=NGE(IE,I1)
      KNUB=NSUB(NLL)
      DO 4 I2=1,NCORN
      LN=NGE(IE,I2)-1
      N4=0
      IF(LN.NE.0) GO TO 74
      GO TO 75
   74 CONTINUE
      DO 11 I=1,LN
   11 N4=N4+NSUB(I)
   75 CONTINUE
      LK=I2-1
      N44=0
      IF(LK.NE.0) GO TO 76
      GO TO 77
   76 CONTINUE
```

```
      DO 14 I=1,LK
   14 N44=N44+KCEM(IE,I)
   77 CONTINUE
      LNN=NGE(IE,I2)
      LNUB=NSUB(LNN)
      DO 4 L1=1,KNUB
      DO 4 L2=1,LNUB
      IF(KNUB.EQ.C) GO TO 4
      IF(LNUB.EQ.0) GO TO 4
      LA=L1+N3
      LB=L2+N4
      IA=L1+N33
      IB=L2+N44
      BMO(LA,LB)=BMO(LA,LB)+SM(IA,IB)
      BKO(LA,LB)=BKC(LA,LB)+SK(IA,IB)
    4 CONTINUE
    1 CONTINUE
      RETURN
      END
```

```
      SUBROUTINE VELDAF (FTLMT,DFTOU,NT,AMAXF,AMINF,AFREE,A,FTCU,KOM,
     *NR,NSET)
      DIMENSION AMAXF(NR,NT),AMINF(NR,NT),AFREE(NR,NT),A(NR,NSET,NT),
     *FTOU(NT)
      READ(5,113) NSET,NR
      READ(5,112) DFTOU,FTLMT
  113 FORMAT(2I3)
  112 FORMAT(8F10.0)
  114 FORMAT(I3)
      DWST=0.05
      NP=1
      READ(5,114) KOM
  247 READ(5,112) S
  253 READ(5,112) R1,R2,ALPHA,BETA
      R2=S+R1-2.0
      FTOU(1)=0.0
      DO 100 I=1,NR
      AMAXF(I,1)=0.0
      AMINF(I,1)=0.0
      AFREE(I,1)=0.0
  100 A(I,NP,1)=0.0
      NI=2
  224 FTOU(NI)=FTOU(NI-1)+DFTOU
      DO 101 I=1,NR
      AMAXF(I,NI)=-4.0
      AMINF(I,NI)=4.0
  101 AFREE(I,NI)=0.0
      WT=0.0
      WTOU=FTOU(NI)*6.28318
      T2=WTOU*S-R2*WTOU
      WST=S*WTOU
      WSTLMT=WST+6.28318
      DWT=WST/100.
      WTR1=WTOU*R1
      WTR2=WTOU*R2
      WST1=WST+WTR2
      WSTLM=WST1+6.28318
      W1DW=1.0/(2.0*FTOU(NI))
      W1=3.14159/WTOU
      W2DW=W1DW/(S-1.0)
      W2=W1/(S-1.0)
      W2TOU=3.14159/(S-1.0)
      W3DW=W1DW/2.0
      W4DW=W2DW/2.0
      IF(ABS(W1DW-1.0).LT.0.0001) GO TO 159
      IF(ABS(W2DW-1.0).GT.0.0001) GO TO 138
  159 DO 131 I=1,NR
      AMAXF(I,NI)=2.0*AMAXF(I,(NI-1))-AMAXF(I,(NI-2))
      AMINF(I,NI)=2.0*AMINF(I,(NI-1))-AMINF(I,(NI-2))
  131 AFREE(I,NI)=2.0*AFREE(I,(NI-1))-AFREE(I,(NI-2))
      GO TO 60
  138 IF(ABS(W3DW-1.0).LT.0.0001) GO TO 159
      IF(ABS(W4DW-1.0).GT.0.0001) GO TO 157
      GO TO 159
  157 AA=W1DW/(1.0-W1DW*W1DW)
      BB=ALPHA/(1.0-W2DW*W2DW)
```

```
      W3TOU=W2TOU/2.0
      CC=1.0/(1.0-W3DW*W3DW)
      DD=1.0/(1.0-W4DW*W4DW)
      GO TO (360,361,362,363,364),KOM
  360 IF(WT.GT.WST) GO TO 210
      AY=-1.0/WTOU+SIN(WT)+COS(WT)/WTOU
      AX=AY
  217 IF(AX.GT.AMAXF(1,NI)) AMAXF(1,NI)=AX
      IF(AX.LT.AMINF(1,NI)) AMINF(1,NI)=AX
      WT=WT+DWT
      GO TO (360,361,362,363,364),KOM
  210 WT=WT+DWST
  261 IF(WT.GT.WSTLMT) GO TO 260
      AX=ABS(COS(WT-WST)*(1.0-S)-COS(WT)+SIN(WT)/WTOU-SIN(WT-WST)/WTOU)
      IF(AX.GT.AFREE(1,NI)) AFREE(1,NI)=AX
      WT=WT+DWST
      GO TO 261
  260 CONTINUE
  216 DO 211 I=1,NR
      AMAXF(I,NI)=ABS(AMAXF(I,NI))
  211 AMINF(I,NI)=ABS(AMINF(I,NI))
      GO TO 60
  361 IF(R1.LT.0.01) GO TO 360
      IF(WT.GT.WST) GO TO 560
      IF(WT.GT.WTR1) GO TO 561
      AY=1.0/WTR1-COS(WT)/WTR1
      AX=AY
      GO TO 65
  561 IF(WT.GT.T2) GO TO 562
      AY=-COS(WT)/WTR1+COS(WT-WTR1)/(WTR1*(1.0-R1))-1.0/(WTOU*(1.0-R1))
      AX=AY
      GO TO 65
  562 CONTINUE
      AY=-COS(WT)/WTR1+COS(WT-WTR1)/(WTR1*(1.0-R1))+COS(WT-T2)*(1.0-S)/(
     1WTR2*(1.0-R1))-(1.0+R2-S)/(WTR2*(1.0-R1))
      AX=AY
   65 CONTINUE
      GO TO 217
  560 AAAAAA=WTR2*(1.0-R1)
      WT4=ATAN((-1.0/WTR1+(1.0-S)*COS(WST-WTR2)/(AAAAAA)+COS(WTR1)/(WTR1
     1-WTR1*R1)-(1.0+R2-S)*COS(WST)/(WTR2-R1*WTR2))/(-(1.0-S)*SIN(WST-WT
     2R2)/(WTR2-R1*WTR2)-SIN(WTR1)/(WTR1-R1*WTR1)+(1.0+R2-S)*SIN(WST)/(W
     3TR2-R1*WTR2)))
      AFREE(1,NI)=ABS(-SIN(WT4)/WTR1+(1.0-S)*SIN(WT4-WST+WTR2)/(WTR2-R1*
     1WTR2)+SIN(WT4-WTR1)/(WTR1-R1*WTR1)-(1.0+R2-S)*SIN(WT4-WST)/(WTR2-R
     21*WTR2))
      GO TO 216
  362 WT1=W1*WT
      WT2=W2*WT
      IF(WT.GT.WST) GO TO 570
      IF(WT.GT.WTOU) GO TO 571
      AY=AA*(COS(WT1)-COS(WT))
      AX=AY
      GO TO 75
  571 CONTINUE
      AY=-AA*(COS(WT)+COS(WT-WTOU))-BB*W2DW*(COS(WT2-W2TOU)-COS(WT-WTOU)
```

```
     1)
      AX=AY
   75 CONTINUE
      GO TO 217
  570 WT=WST+DWST
  574 IF(WT.GT.WSTLMT) GO TO 573
      WT1=W1*WT
      AX=ABS(-AA*(SIN(WT)+SIN(WT-WTOU))-BB*(-W2DW*SIN(WT-WTCU)+SIN(W2TCU
     1*S-W2TOU)*COS(WT-WST)+W2DW*COS(W2TOU*S-W2TOU)*SIN(WT-WST)))
      IF(AX.GT.AFREE(1,NI)) AFREE(1,NI)=AX
      WT=WT+DWST
      GO TO 574
  573 CONTINUE
      GO TO 216
  363 WT1=W1*WT/2.0
      WT2=W2*WT/2.0
      IF(WT.GT.WST) GO TO 580
      IF(WT.GT.WTOU) GO TO 581
      AY=CC*(-W3DW*SIN(WT1)+SIN(WT))
      AX=AY
      GO TO 85
  581 CONTINUE
      AY=CC*(SIN(WT)-W3DW*COS(WT-WTOU))-DD*ALPHA*W4DW*(COS(WT2-W3TOU)-CO
     1S(WT-WTOU))
      AX=AY
   85 CONTINUE
      GO TO 217
  580 WT=WT+DWST
  584 IF(WT.GT.WSTLMT) GO TO 583
      WT2=W2*WT/2.0
      AX=ABS(CC*(-COS(WT)-W3DW*SIN(WT-WTOU))-DD*ALPHA*(-W4DW*SIN(WT-WTOU
     1)+COS(WT-WST)))
      IF(AX.GT.AFREE(1,NI)) AFREE(1,NI)=AX
      WT=WT+DWST
      GO TO 584
  583 CONTINUE
      GO TO 216
  364 IF(WT.GT.WST1) GO TO 590
      IF(WT.GT.WTR1) GO TO 591
      AY=-(1.0-ALPHA*(1.0-R1))/WTR1+SIN(WT)+(1.0-ALPHA*(1.0-R1))*COS(WT)
     1/WTR1
      AX=AY
      GO TO 217
  591 IF(WT.GT.WST) GO TO 592
      AY=-ALPHA/WTOU+(1.0-ALPHA*(1.0-R1))*COS(WT)/WTR1+SIN(WT)-(1.0-ALPH
     1A)*COS(WT-WTR1)/WTR1
      AX=AY
      GO TO 217
  592 CONTINUE
      AY=-(1.0-S-BETA/ALPHA)*ALPHA*SIN(WT-WST)+(1.0-ALPHA*(1.0-R1))*COS(
     1WT)/WTR1+SIN(WT)-(1.0-ALPHA)*COS(WT-WTR1)/WTR1+(BETA-ALPHA*R2)*COS
     2(WT-WST)/WTR2-BETA/WTR2
      AX=AY
      GO TO 217
  590 WT=WST1+DWST
  594 IF(WT.GT.WSTLM) GO TO 593
```

```
      AX=ABS(( 1.0-S-BETA/ALPHA)*ALPHA*COS(WT-WST)+(1.C-ALPHA*(1.C-R1))*
     1SIN(WT)/WTR1-COS(WT)-(1.0-ALPHA)*SIN(WT-WTR1)/WTR1+(BETA-ALPHA*R2)
     2*SIN(WT-WST)/WTR2-BETA*SIN(WT-WST-WTR2)/WTR2)
      IF(AX.GT.AFREE(1,NI)) AFREE(1,NI)=AX
      WT=WT+DWST
      GO TO 594
  593 CONTINUE
      GO TO 216
   60 DO 212 I=1,NR
      IF(AMAXF(I,NI).GT.AMINF(I,NI)) GO TO 31
      IF(AMINF(I,NI).GT.AFREE(I,NI)) GO TO 32
      GO TO 33
   31 IF(AMAXF(I,NI).GT.AFREE(I,NI)) GO TO 34
      GO TO 33
   32 A(I,NP,NI)=AMINF(I,NI)
      GO TO 35
   33 A(I,NP,NI)=AFREE(I,NI)
      GO TO 35
   34 A(I,NP,NI)=AMAXF(I,NI)
   35 CONTINUE
  212 CONTINUE
      WRITE(6,400) FTOU(NI),AMAXF(NR,NI),AMINF(NR,NI),AFREE(NR,NI),
     *A(NR,NP,NI)
  400 FORMAT(5F15.6)
      IF(FTOU(NI).GT.FTLMT) GO TO 225
      NI=NI+1
      GO TO 224
  225 CONTINUE
      NP=NP+1
      IF(NP.GT.NSET) GO TO 249
      GO TO 247
  249 CONTINUE
      RETURN
      END
```